Validation and Pilot Applications of Unsteady CFD Simulations for the Analysis of Propeller Flows

High Performance Computing
and Networking Workshop
September 25th/26th, 2008
DLR Braunschweig

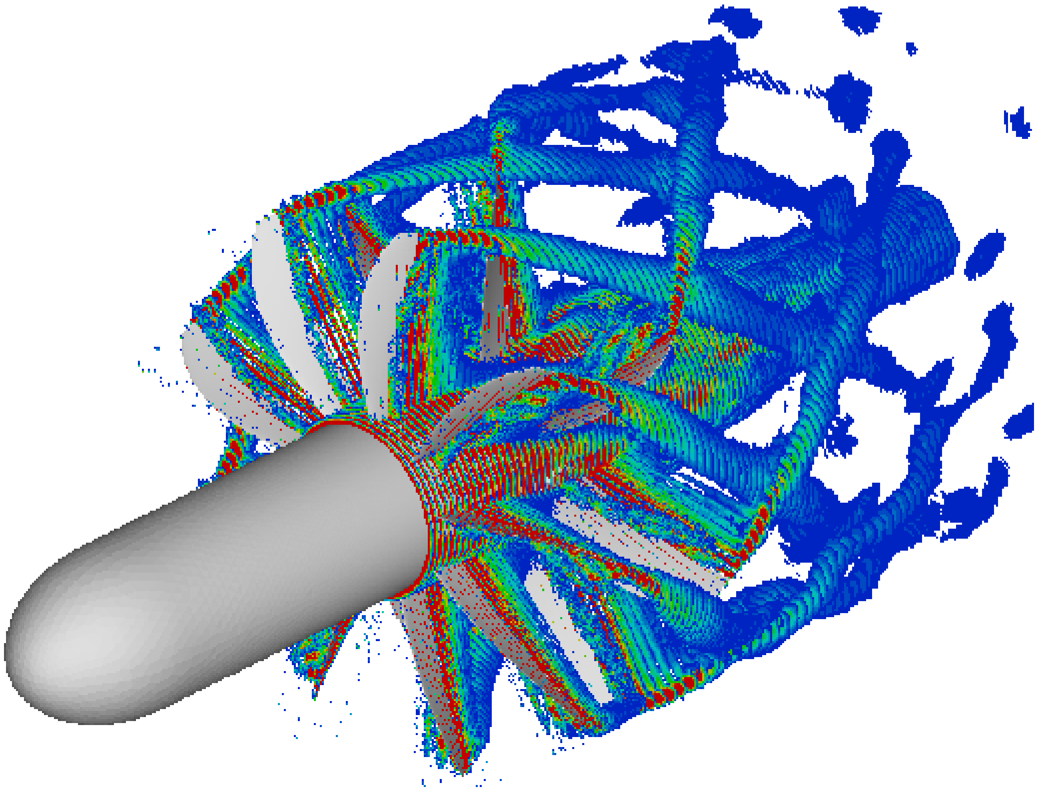

Arne Stuermer
Institute of Aerodynamics
and Flow Technology
DLR Braunschweig

Deutsches Zentrum
für Luft- und Raumfahrt e.V.
in der Helmholtz-Gemeinschaft

Overview

- Introduction and Motivation:
  - Why Propellers & why HPC?
- Software Tools and Approaches
- Example Applications
  - Aims, CAD, CFD and Analysis
    - Gen-Av: 6th EU FP IP CESAR
    - Contract Work: Military Transport Aircraft
      - Omitted from distribution @ contractor request
    - CROR – a Future Commercial Aviation Propulsion System?
- Conclusion and Outlook
  - HPC benefits for Propeller Simulations

Introduction and Motivation: Simulation of the Rotating Propeller

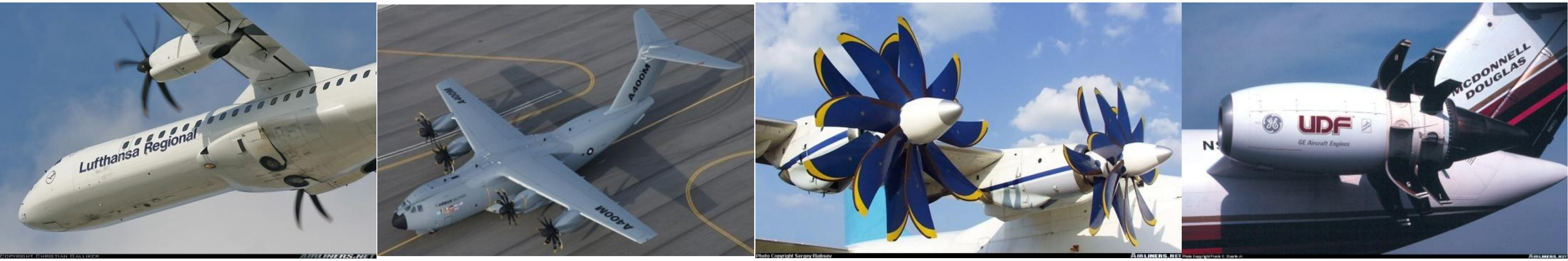

- Propellers remain an attractive form of aircraft propulsion due to their superior efficiency and/or their performance characteristics for tactical military transport missions
- Cost of fuel has lead to a renaissance of the Propfan (GE-UDF, NASA ATP), aka Contra-Rotating Open Rotor (CROR)/Contra-Rotating Propeller (CRP)
- Complex aerodynamic interactions require careful engine-airframe integration design
- Why expensive (unsteady) simulation of the rotating propeller?
  - Compute unsteady interactions of propeller and airframe without simplifications or assumptions
  - Only possibility of obtaining propeller blade loads directly with CFD
  - Input/validation data for simpler computational methods (actuator disc)
  - Unsteady aerodynamic data can form basis for detailed aero acoustic and vibroacoustic/structural analysis

Simulation of the Rotating Propeller: The DLR TAU CFD-code

- Requirements for unsteady rotating propeller CFD:
  - Capability of modeling multiple rigid bodies in relative motion
  - Time-accurate simulation
- The DLR TAU-Code:
  - Unstructured finite volume Euler/RANS-flow solver
  - All standard state-of-the-art CFD techniques available:
    - Central and upwind schemes for spatial discretization
    - Matrix dissipation
    - Multistage Runge-Kutta time-stepping, LUSGS
    - Convergence acceleration through MG, residual smoothing, local time-steps
    - 1- and 2-equation turbulence models (SAE,k-ω SST)
    - Rotational/Vortical correction
  - Chimera Grid approach + motion libraries
  - Dual time stepping scheme for unsteady computations

Gen-Av: 6th FP IP CESAR: Aerodynamic and Aeroacoustic Analysis of Pusher Propeller Configurations

High Performance Computing and Networking Workshop
September 25th/26th, 2008
DLR Braunschweig

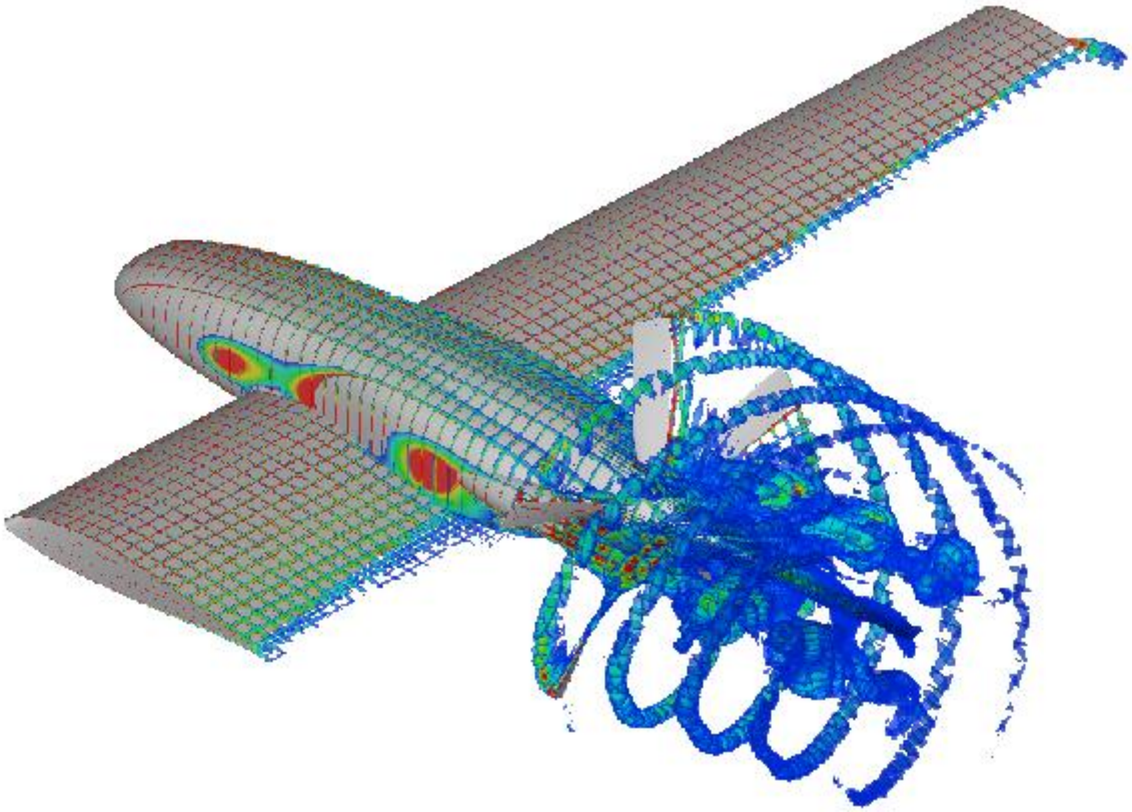

Arne Stuermer &
Dr. Jianping Yin
Institute of Aerodynamics and Flow Technology
DLR Braunschweig

Deutsches Zentrum
für Luft- und Raumfahrt e.V.
in der Helmholtz-Gemeinschaft

CESAR: Overview, Geometry & Meshing

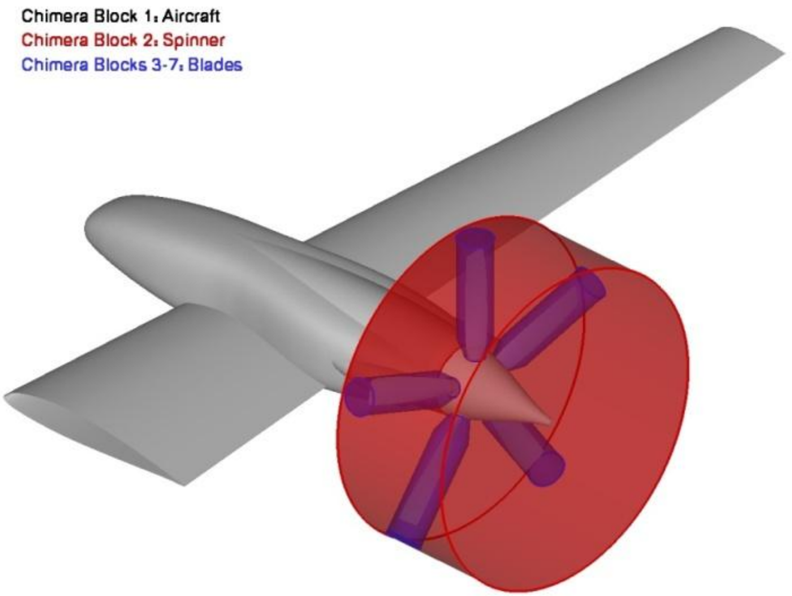

- Cost Effective Small AiRcraft
- DLR-AS active in Piaggio-led task focused on analysis of aerodynamics and aeroacoustics of Piaggio P180 Avanti II derived pusher propeller configuration
- Coupled DLR TAU and APSIM analysis with both actuator disc modesl and rotating propeller with engine jet simulation

- Full flexibility of Chimera approach exploited in using 7 mesh blocks
- Mesh generation using CentaurSoft Centaur
- Special care taken during CAD setup and mesh generation to ensure adequate discretization in overlap areas
- Full grid with 31.166.768 nodes

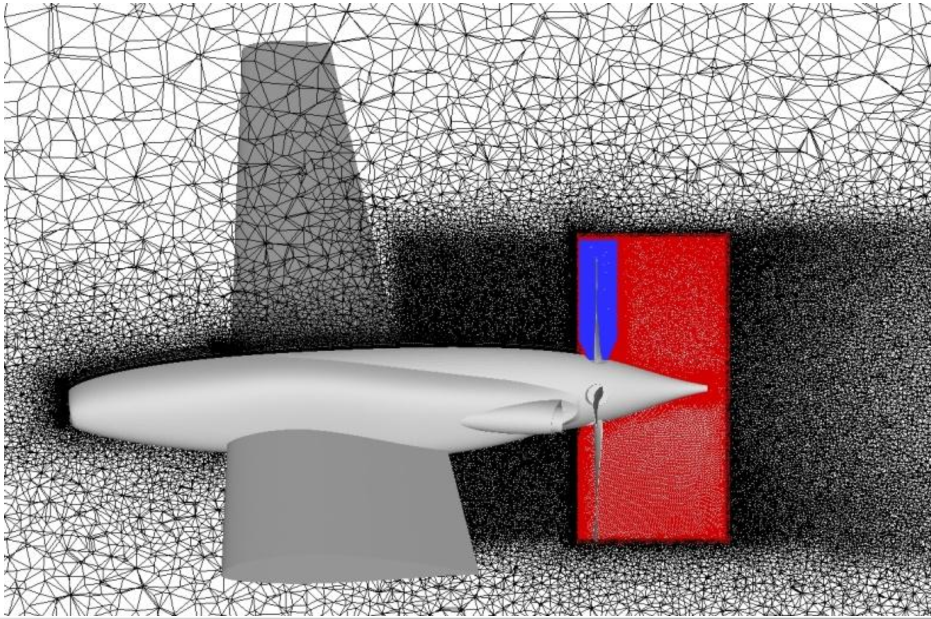

CESAR:
Test Case Definition

- Simulation of a high power setting climb case
- h=400 ft, M=0.235, α=6.5º
- Engine setting: P=850shp/634kW @ 2000rpm, J=1.101
- Manufacturer specs:
  - $p_{t,7}$=108070 N/m^2, $T_{t,7}$=831 K, m=4.1173 kg/s, v_7=193 m/s

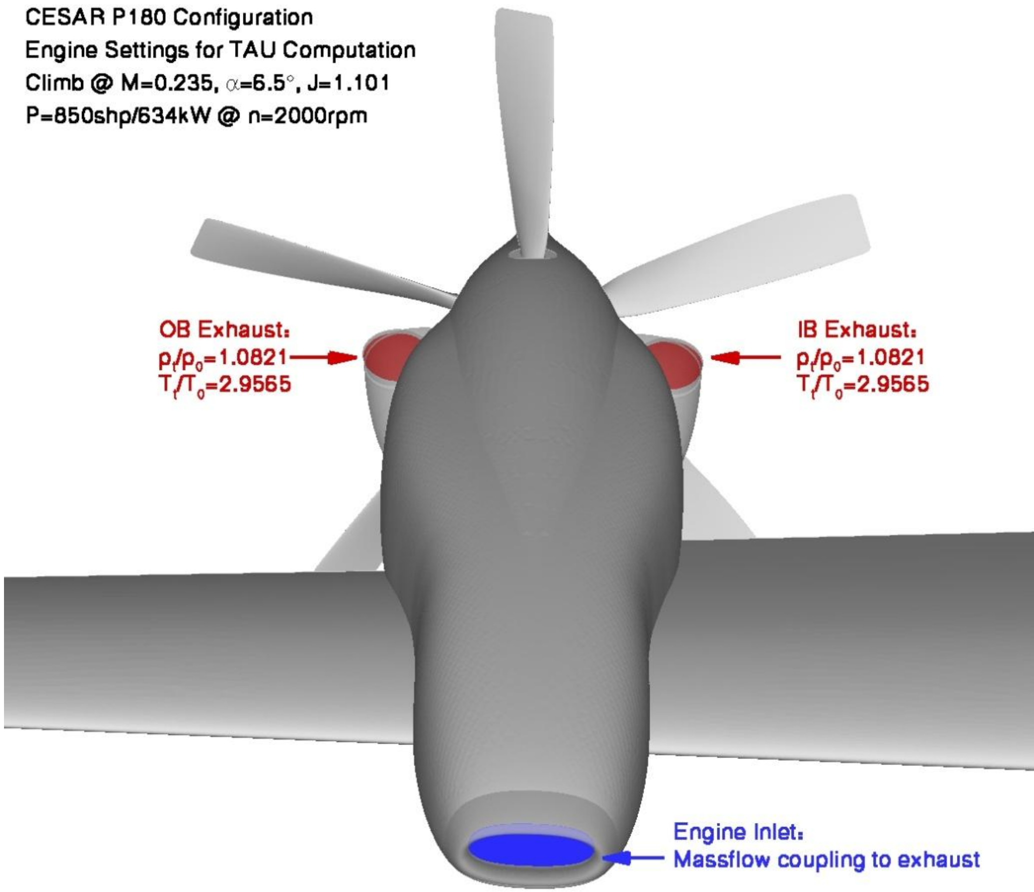

CESAR:
Computational Approach

- Computations run on 48-96 CPUs of various DLR clusters (585.6h/24.4d)
- Steady computation with blades pitched to β_{75}=90º to stabilize engine model start-up
- Initiation of uRANS computation form steady solution with blades pitched to specified angle of β_{75}=32.5º and propeller rotation of n=2000rpm
- Use of central discretization, matrix dissipation, 3V-MG cycle, fully turbulent computation (sorry, Piaggio) with SAE turbulence model
- Start-up with prop-rotation of dψ=8º per physical time-step, subsequent reduction in steps to dψ=2º
- Use of 200 inner iterations

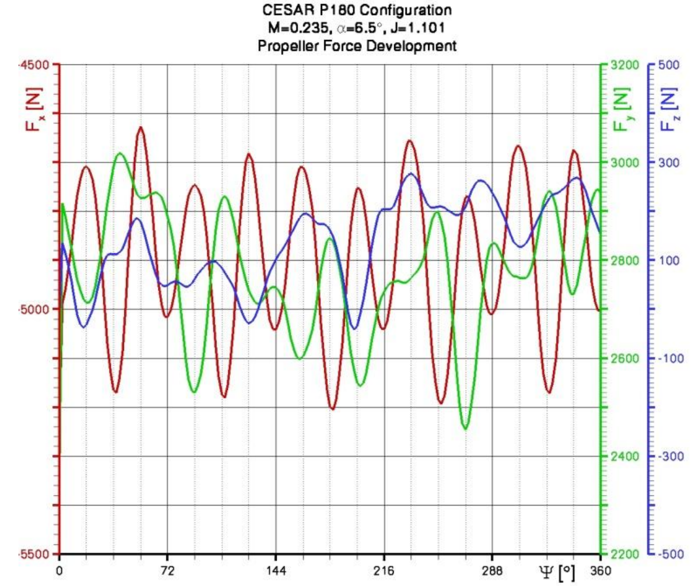

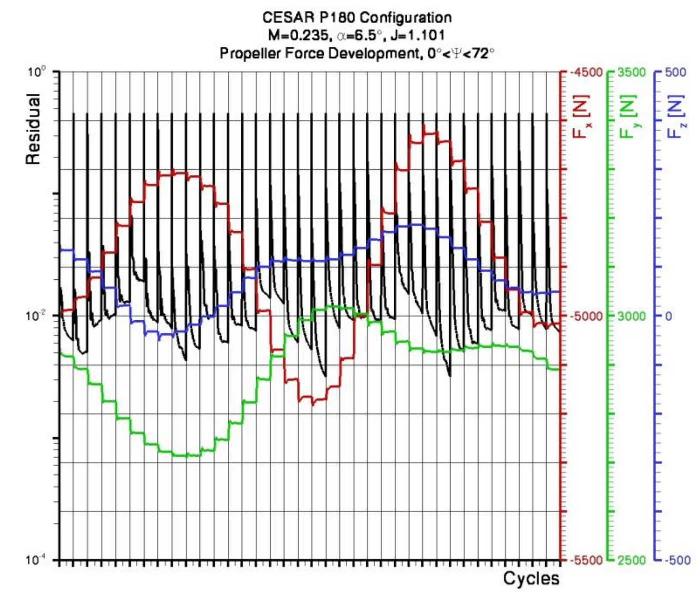

CESAR: Prop-Jet-Interactions

- Close proximity of exhaust and propeller plane leads to strong mutual interactions
- Propeller blades “slice” and deflect the jets during their rotation
- Entrainment of engine jet in swirl of propwash
- Blade passage in front of exhausts causes pressure fluctuations at the outlet

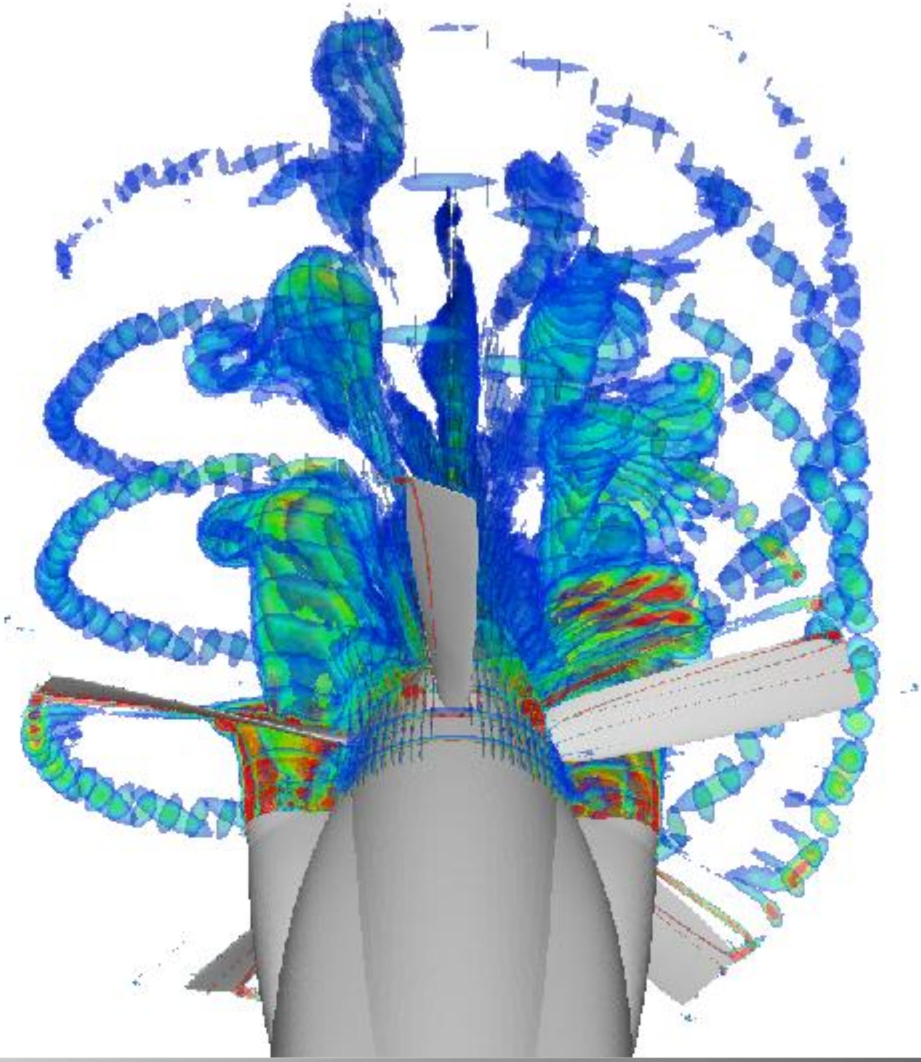

Deutsches Zentrum für Luft- und Raumfahrt e.V. in der Helmholtz-Gemeinschaft

CESAR: Propeller-Jet-Interactions

- Section r/R=0.4 is directly affected by the engine jets
- During blade passage in front of exhaust, jet velocities lead to a significant reduction in local blade AoA
- Notable suction peaks occur on blade PS LE during passage
- Local loss in thrust

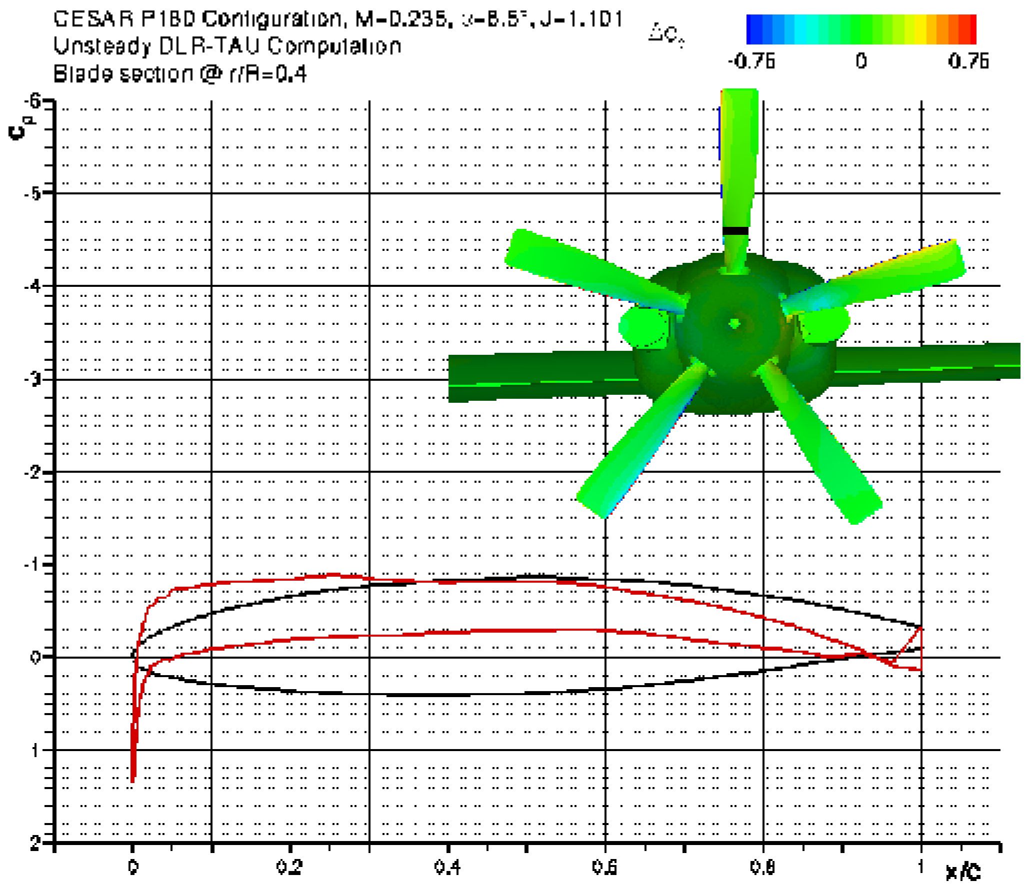

CESAR:
Propeller-Jet-Interactions

- Blade force distribution shows impact of aircraft AoA
- Strong local impact during interaction with engine jets visible
- A radial influence of the propeller-jet interaction effect can be seen
- More detailed analysis of flow field needed to determine wing wake impact (if grid resolution was sufficient)

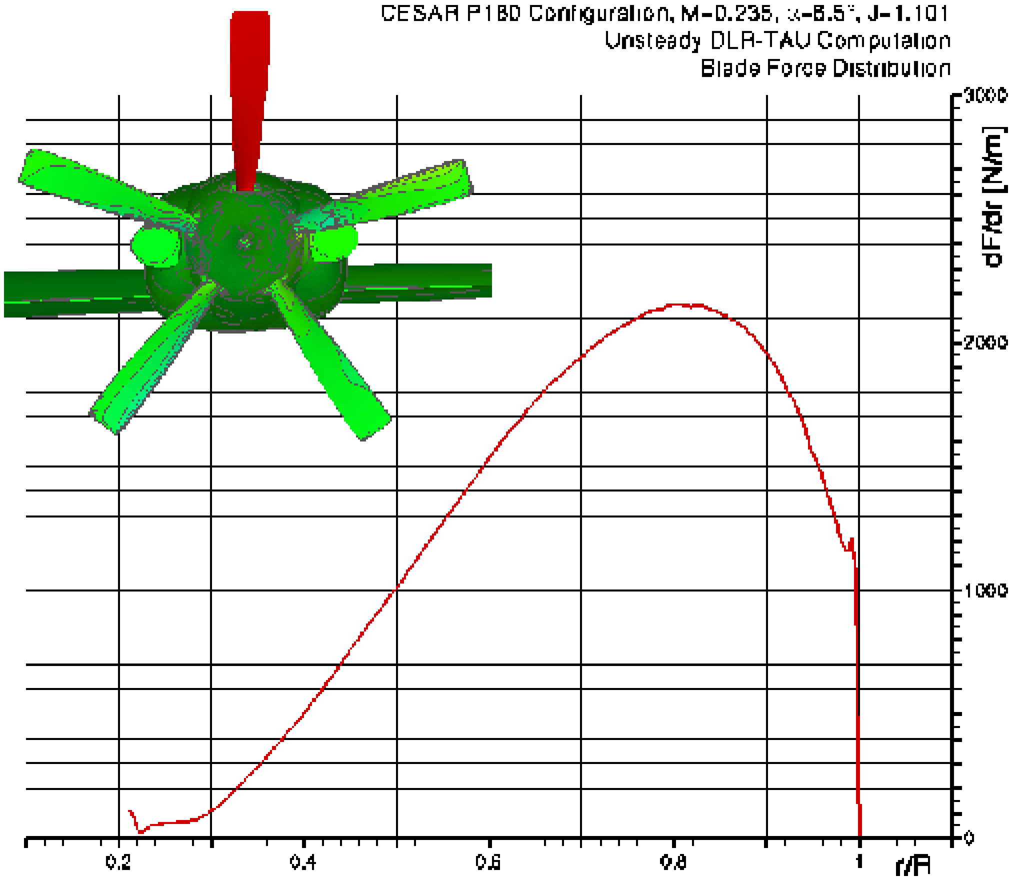

CESAR:
Propeller Force Development

- Blade forces show overlapping impact of AoA and interaction with engine jet (and wing wakes)
- Pronounced periodic fluctuations for propeller force components
- Lower thrust (-22%) than isolated propeller reference data
- Lower propeller torque (-23%), i.e. less power: P=651.8 shp/486 kW
- Better efficiency (+1.14 %-points)
  - Cause: Installation effects + less blade twist than in spec?

	F_X [N]	C_T	C_Y	C_Z	C_l	η
Blade	**974.6776**	**0.0332784**	**0.0008487**	**0.0012074**	**0.000260**	**-**
Propeller	**4893.1835**	**0.1670678**	**0.0030637**	**0.0065258**	**0.0366815**	**79.80%**

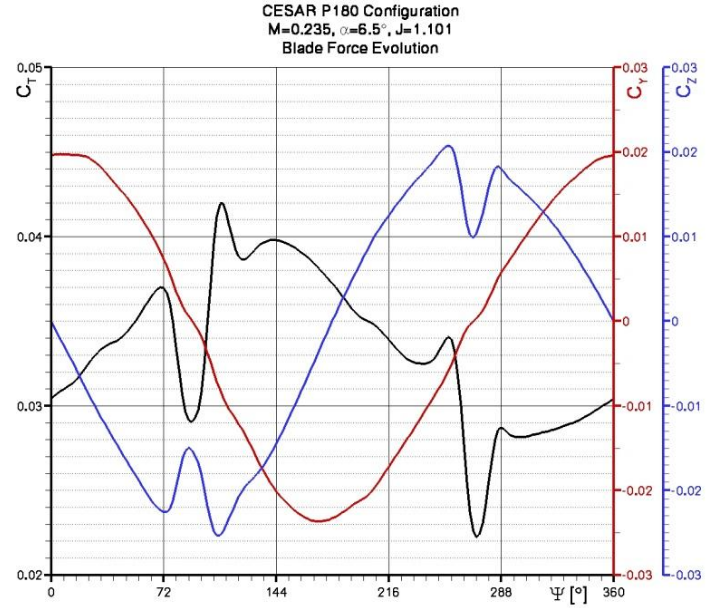

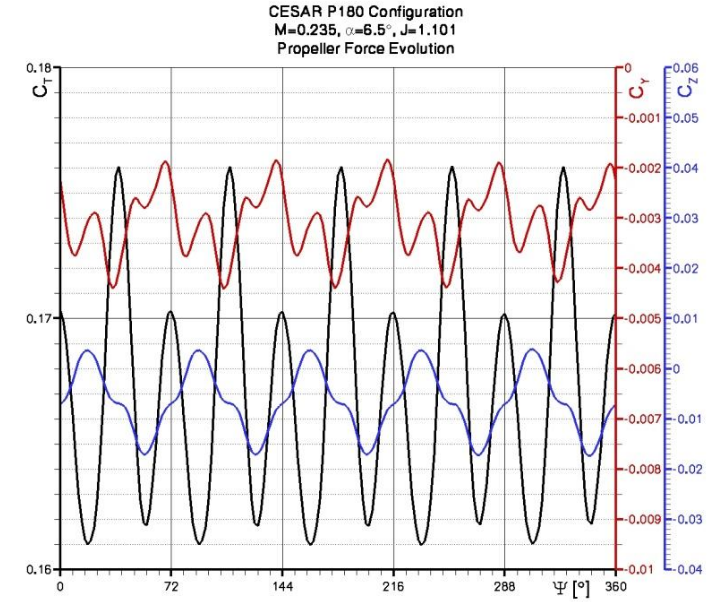

CESAR: Propeller-Airframe-Interactions

- Notable interaction of propeller with upstream aircraft is evident
- Pressure fluctuations visible on the wing
  - Pronounced in region directly in front of propeller
  - Diminishing but notable impact on remainder of the configuration

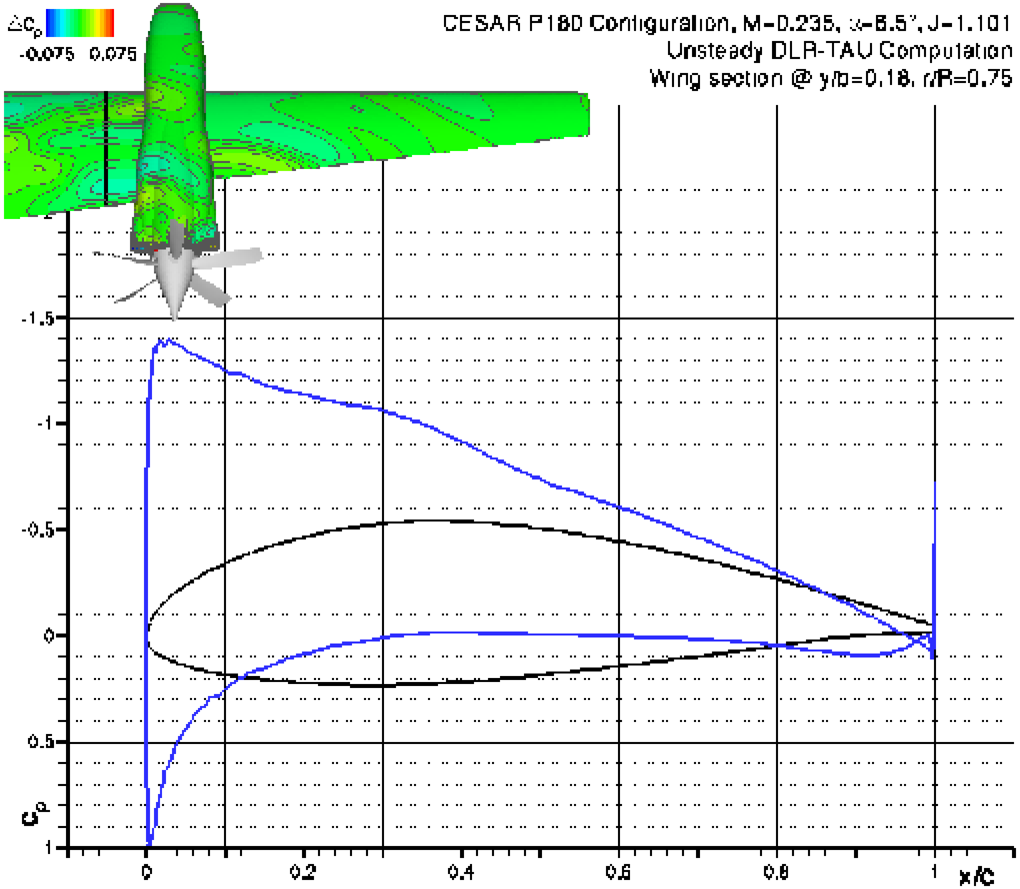

CESAR:
Propeller-Airframe-Interactions

- Spanwise lift distribution shows clear interactions with propeller flowfield
- Pronounced periodic oscillations in phase with blade passage seen on IB wing, nacelle, IB anc OB exhaust fairings and diminishing towards the tip on the OB wing

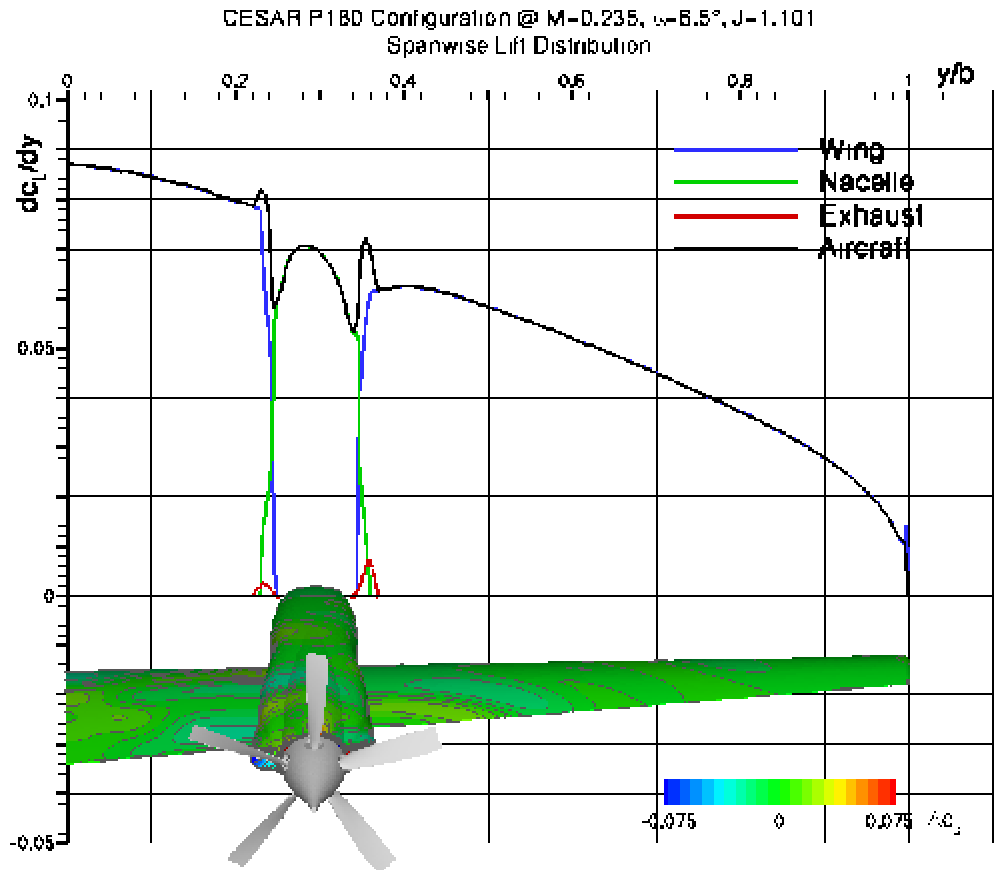

CESAR: Aeroacoustic Analysis Tools and Approaches

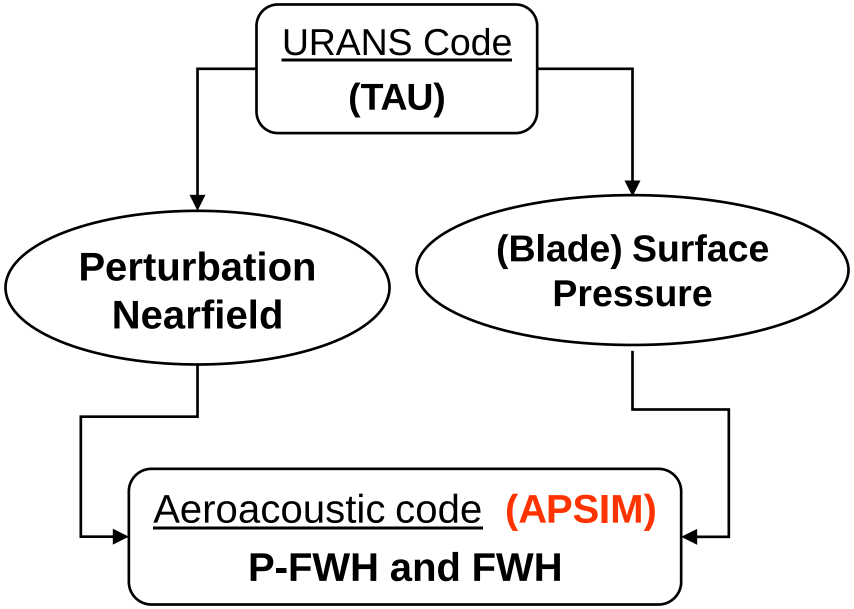

Hybrid method

TAU

→ acoustic near-field (source region) or (Blade) surface pressure

APSIM

→ acoustic far-field

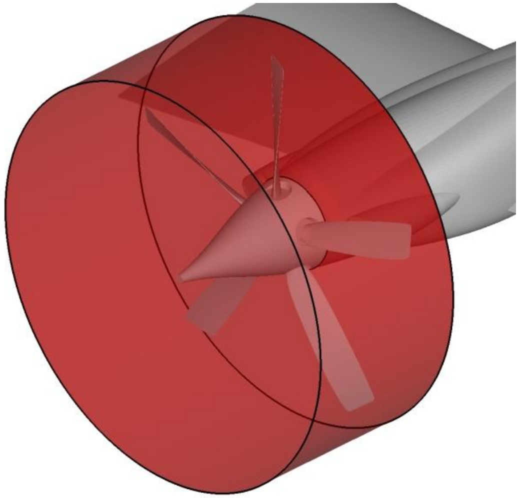

APSIM (Acoustic Prediction System based on Integral Method)

- Noise Prediction of Rotors and Propellers
- Linear Acoustic Analogy Method
- Permeable or **Non-Permeable (blade surface) FW-H**
- Kirchhoff Method
- **Rotating and** Non-rotating **Surface**

CESAR: Aeroacoustics

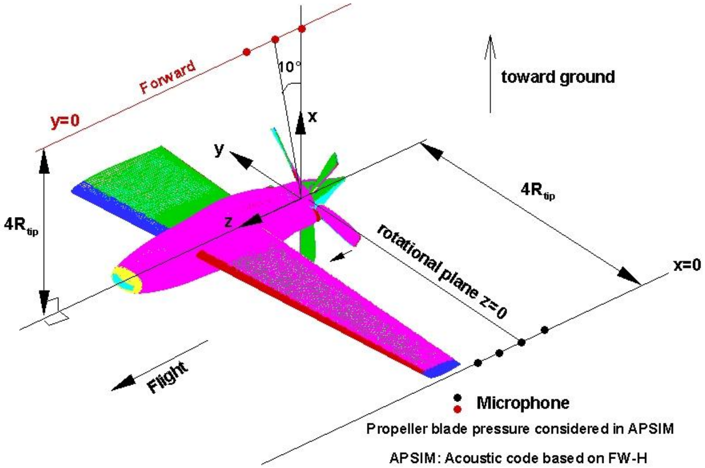

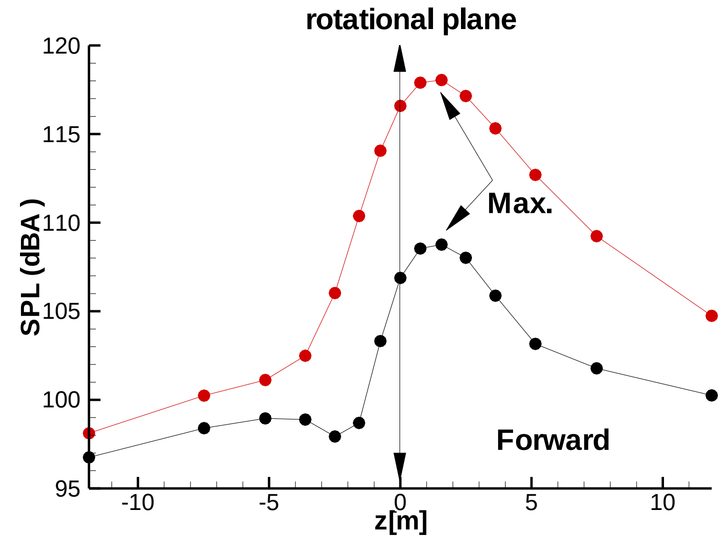

Predicted Noise Level as Function of Directivity

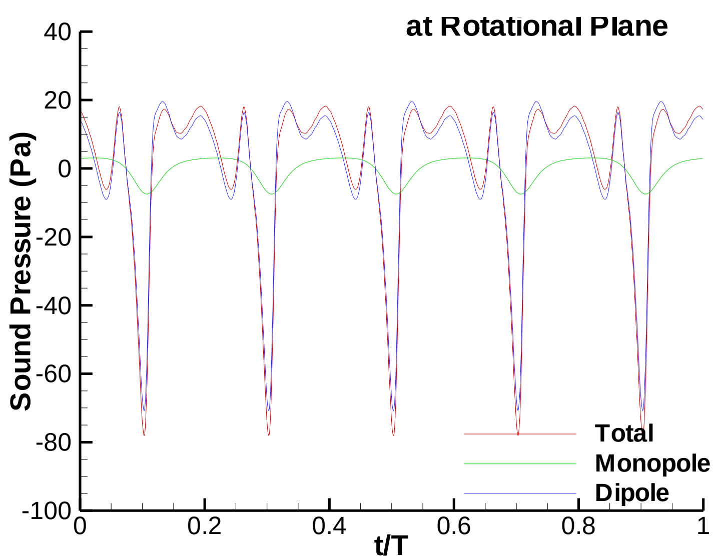

Sound Pressure as Function of Revolution

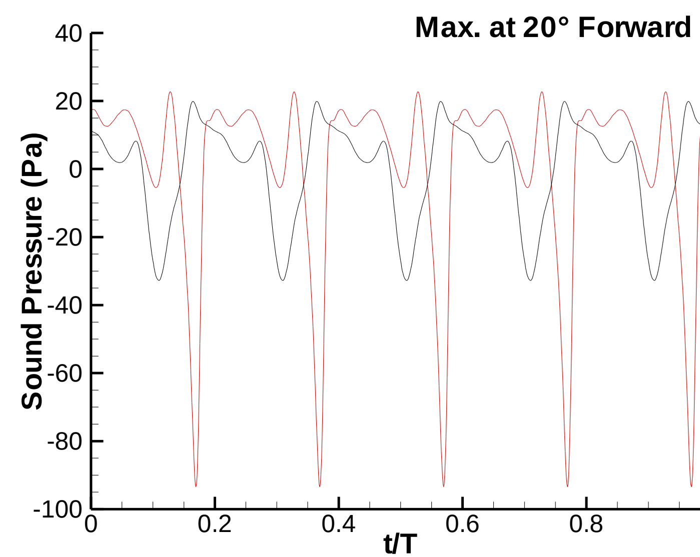

Sound Pressure as Function of Revolution

CESAR:
Conclusion & Outlook

- Promising results achieved which show benefit of high-fidelity approach to this type of analysis as it allows for very detailed understanding of the physical phenomena

- Future work in CESAR will focus on identification of noise reduction potential of altering engine exhaust geometries
- Other partners have designed a new 6-bladed propeller
- All work in WP3.3 will lead to flight test of optimized configuration on the P.180 Avanti II

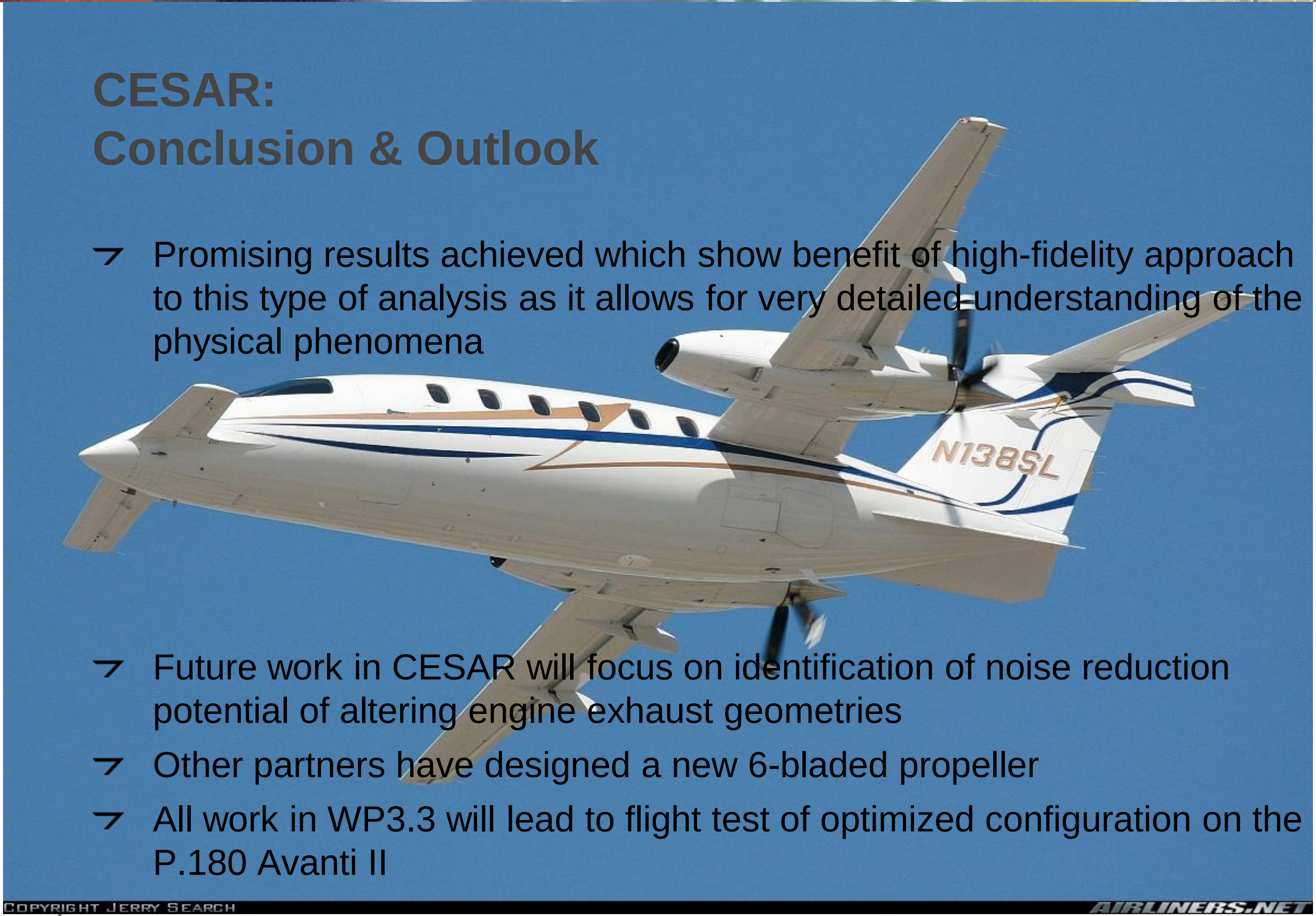

Contract Work: uRANS Simulation of Propeller-Aircraft Interaction Effects for Military Transport Aircraft in High-Lift Configuration

High Performance Computing
and Networking Workshop
September 25th/26th, 2008
DLR Braunschweig

Omitted from open distribution at contractor request

Arne Stuermer
Institute of Aerodynamics
and Flow Technology
DLR Braunschweig

Deutsches Zentrum
für Luft- und Raumfahrt e.V.
in der Helmholtz-Gemeinschaft

Military Transport Aircraft: Conclusion & Outlook

- Omitted from open distribution at contractor request

- First large-scale application of propeller simulation experience with TAU to fully realistic and very complex geometry
- Favorable agreement with comprehensive experimental database, with most differences most likely attributable to simplified inviscid modeling of blades
- Highlight of potential additional benefits of hi-fi uRANS Simulations:
  - Vibro-acoustics, Sonic fatigue, Aeroacoustics
- Lessons learned flowing into all current work, including another similar computation for a different thrust setting:
  - Despite larger mesh due to viscous modeling of blades, completion expected in maybe <1/3 of the time (partly CASE, partly approach)

CROR Numerical Test Rig: Development of Tools, Methods and Approaches for CROR Simulations

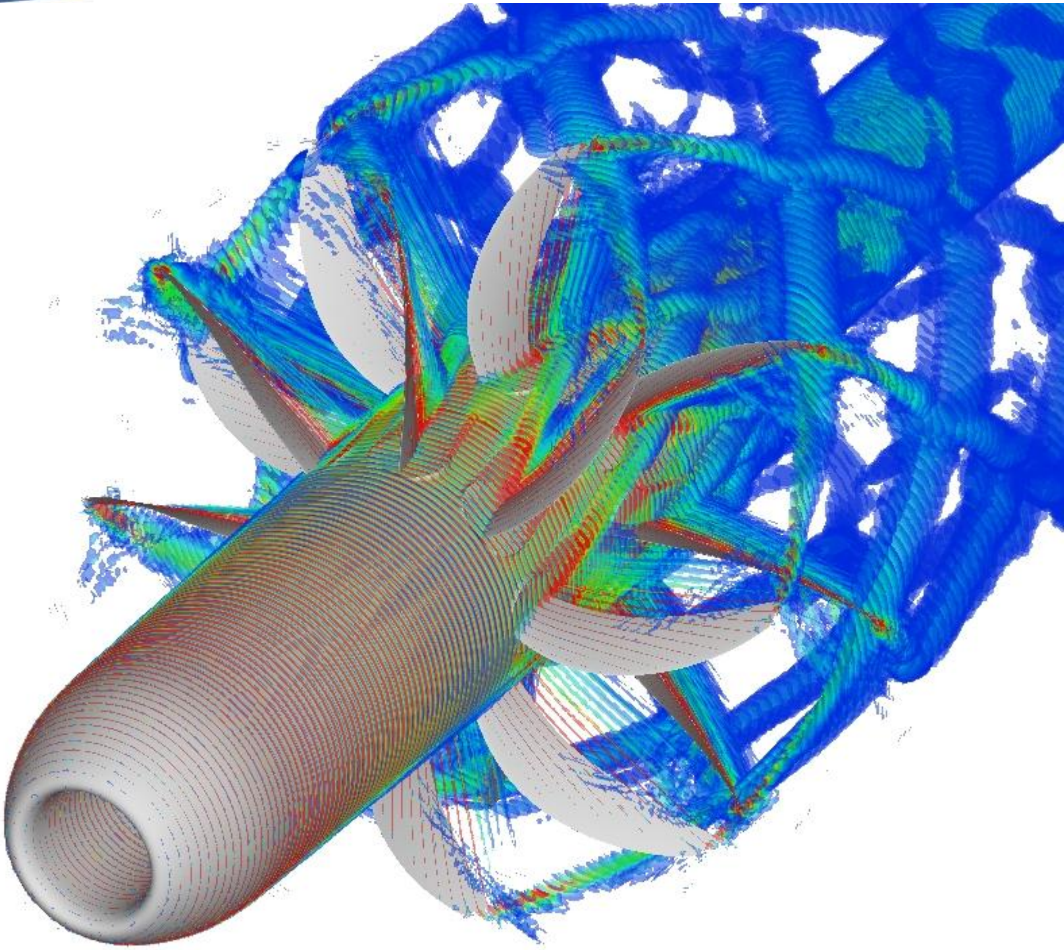

Adapted from:
Paper AIAA 2008-5218
44th AIAA/ASME/SAE/ASEE Joint Propulsion Conference & Exhibit
Hartford, CT, USA
July 23rd, 2008

Arne Stuermer
Institute of Aerodynamics and Flow Technology
DLR Braunschweig

DLR Deutsches Zentrum für Luft- und Raumfahrt e.V.
in der Helmholtz-Gemeinschaft

CROR Numerical Test Rig: Introduction and Motivation



- Cost of fuel has lead to a renaissance of the Propfan, aka Contra-Rotating Open Rotor (CROR)
- 1973 oil crisis motivated the NASA/US Industry Advanced Turboprop Project (ATP) , which conducted comprehensive research on CROR aerodynamics and aeroacoustics, culminating in flight tests of two prototype engines on the McDonnell Douglas MD-80 and Boeing 727
- Propfans almost made it into service in late ’80s/early ’90s with versions of the GE36-UDF or P&W/Allison 578-DX on the proposed McDonnell Douglas MD-90XX and Boeing 7J7 aircraft
- Drop in fuel prices lead to waning of interest in the demonstrated efficiency advantages, which still had issues relating to noise, integration, certification to be solved in product development
- Today, costs of fuel are eating into airline profits again (‘08: 33% of TOC; ’98:9.4% of TOC), so CRORs are back on the table
- Installation, noise and certification issues still remain:
  - Modern methods could play vital role in realizing full potential of CRORs for EIS ~2020
  - Consensus: CROR could be up to 15% better in SFC than equivalent technology “advanced turbofans”

CROR Numerical Test Rig: Geometry

- Generic 8x8 Pusher Configuration as Baseline Design
- Aimed at 150-seat commercial transport segment (TO-thrust ~20,000lfb/88kN, cruise thrust ~4250lbf/19kN)
- Propeller diameter D=14ft/4.2672m
- Nacelle design borrows from the GE36 UDF
- Hub-to-Tip ratio selected as d/D=0.355
- Flexible & modular geometry design in CATIA V5

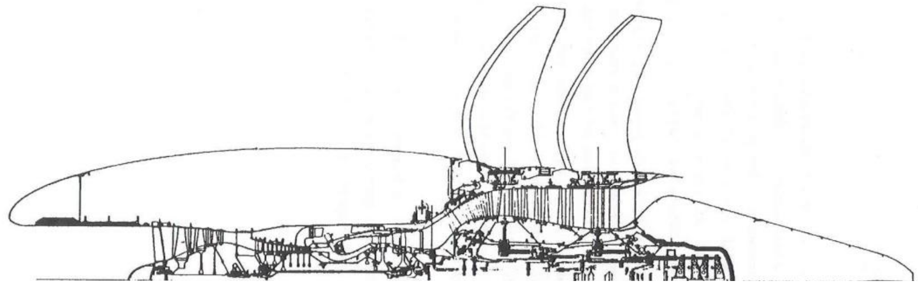

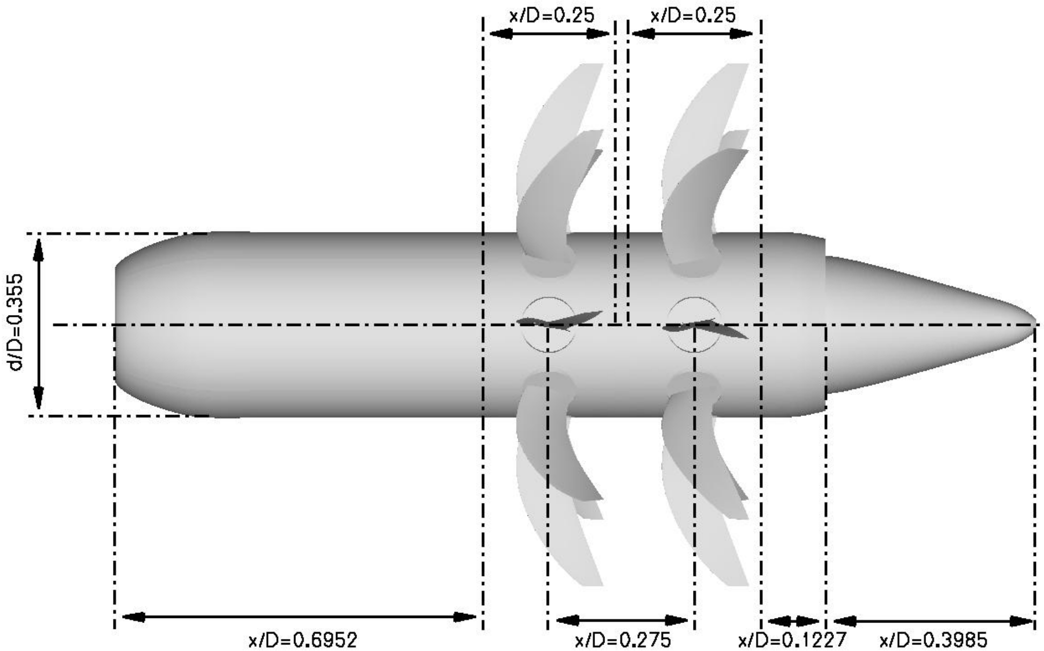

CROR Numerical Test Rig: Blade Design

- Baseline blade designed for use in both of the 8-bladed rotors
- SRP design for CRP use:
  - First shot guess of similar performance in both rotors, approximately equal thrust
- Airfoil selection and design strategy similar to ATP project approach
- Blade element theory and TAU RANS simulations
- Purely aerodynamic design
  - Similar characteristics to other blades
  - Minimum tip t/c=0.03

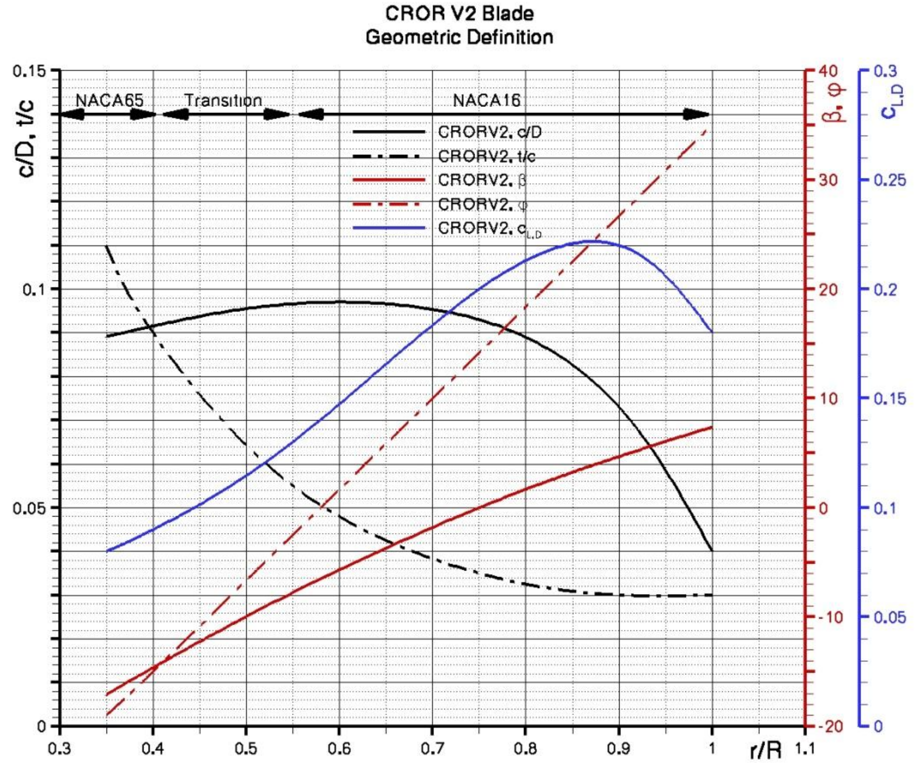

CROR Rig: Blade Design

- Blade design performance and flow topology satisfactory
- Cruise:
  - C_T = 0.33 (F_x = 9.358kN) with η=77.43% at β_{75} = 60º
  - Best efficiency around η=77.73%
- Take-Off:
  - C_T = 0.395 (F_x = 44.906kN) with η=58.21% at β_{75} = 36º

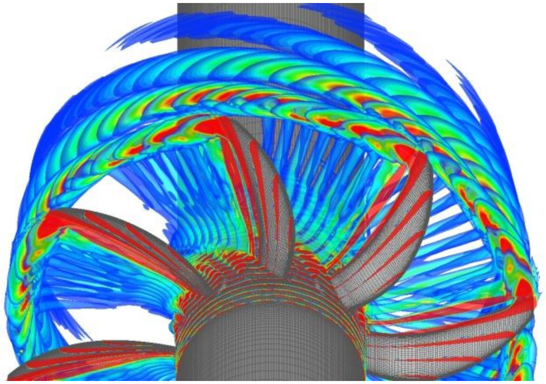

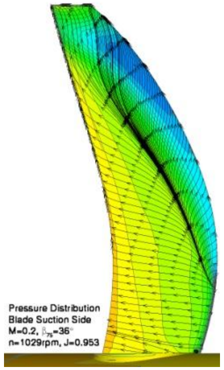

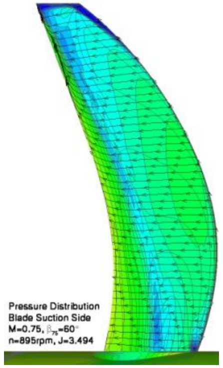

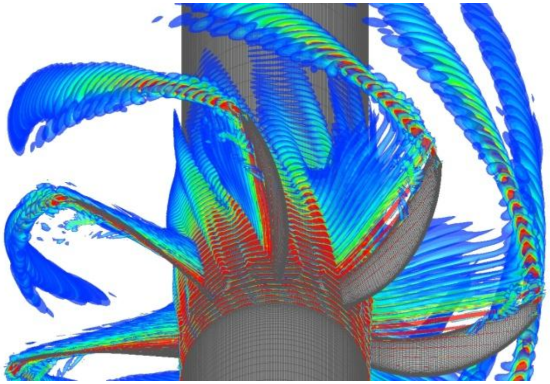

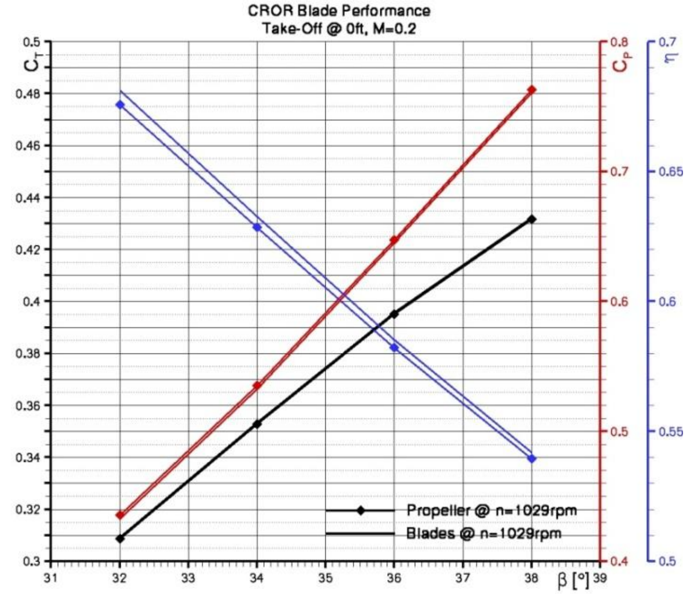

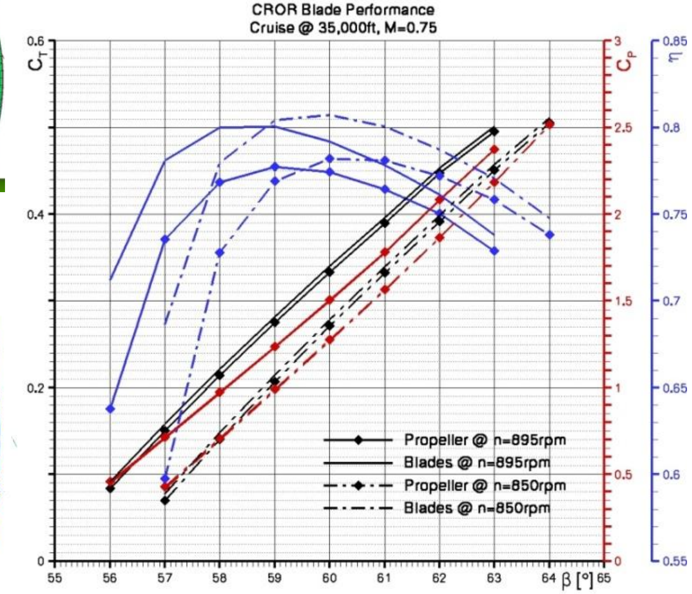

CROR Numerical Test Rig: Geometry & Mesh Generation

- Unstructured/structured mesh generation with CentaurSoft Centaur and ICEM CFD HEXA
- 20 mesh blocks used to fully exploit flexibility of Chimera approach
- Symmetry exploited
- Nacelle and rotor block:
  - 45° segment meshed and subsequently completed to full configuration

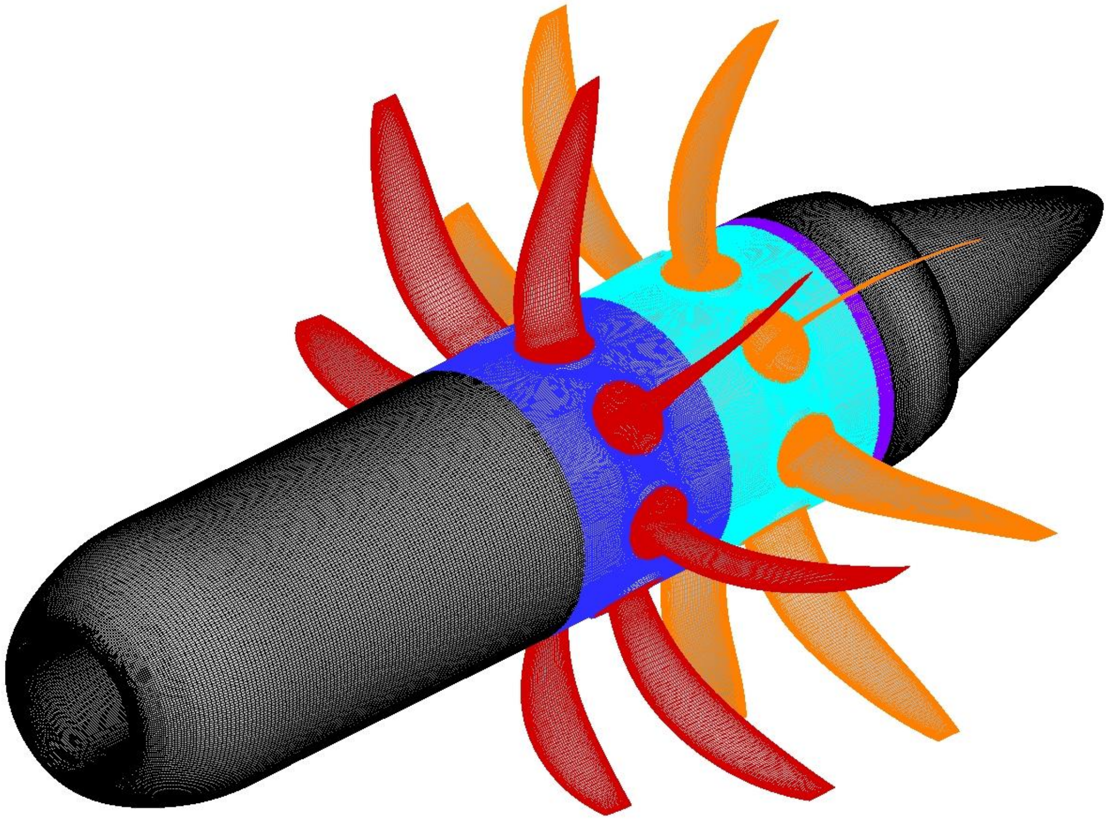

CROR Numerical Test Rig: Geometry & Mesh Generation

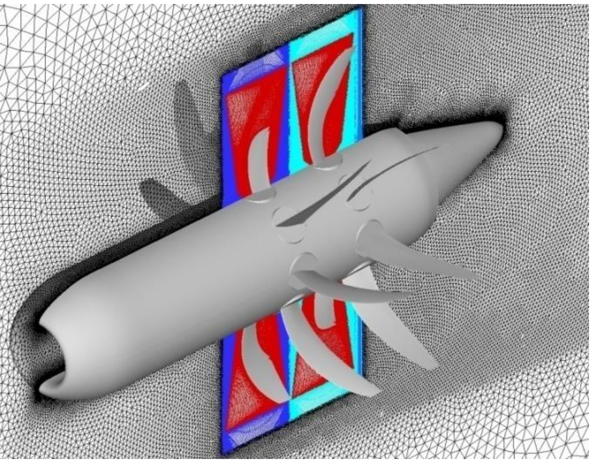

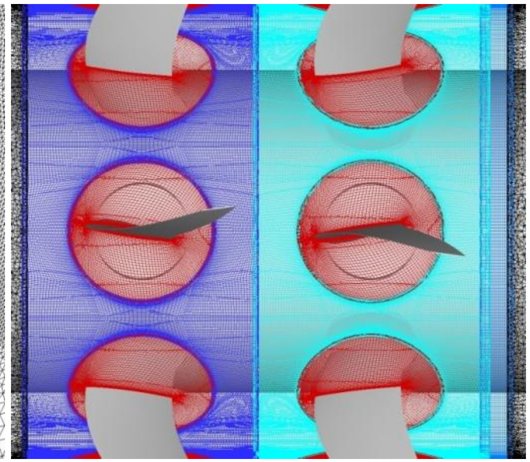

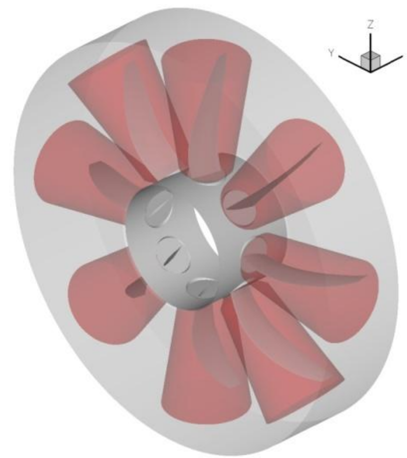

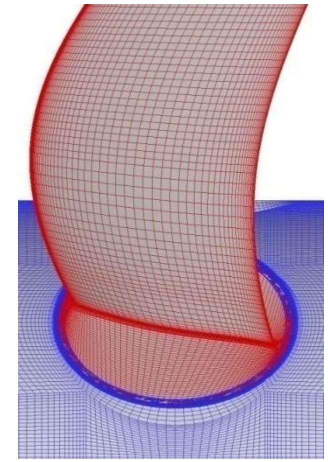

- Hub PCM geometry introduced to allow flexible adjustment of blade pitch angles
- One structured blade mesh generated, common to both rotors
- Special care taken to ensure Chimera overlap regions are adequate
- Initial cell spacing near surfaces adapted for appropriate viscous sublayer resolution (y+~1)
- Rotor Chimera boundary can serve as interface to aeracoustic tools
- Total mesh size: 40,000,000 nodes

CROR Numerical Test Rig: Test Case Definition

- Cruise conditions for flight at M=0.75 and h=35,000ft
- 2 AoAs: α=0º and α=2º
- Identical propeller rotational speeds of n=895rpm (J=3.494)
- Use of TAU engine boundary condition to simulate generic but realistic inlet and jet flow fields
  - Specification of total to static pressure and total to static temperature on outlet plane; massflow coupling for inflow plane
- Blade pitch for a 50:50 thrust split:
  - $\beta_{75,R1}$=61° and $\beta_{75,R2}$=57.9°

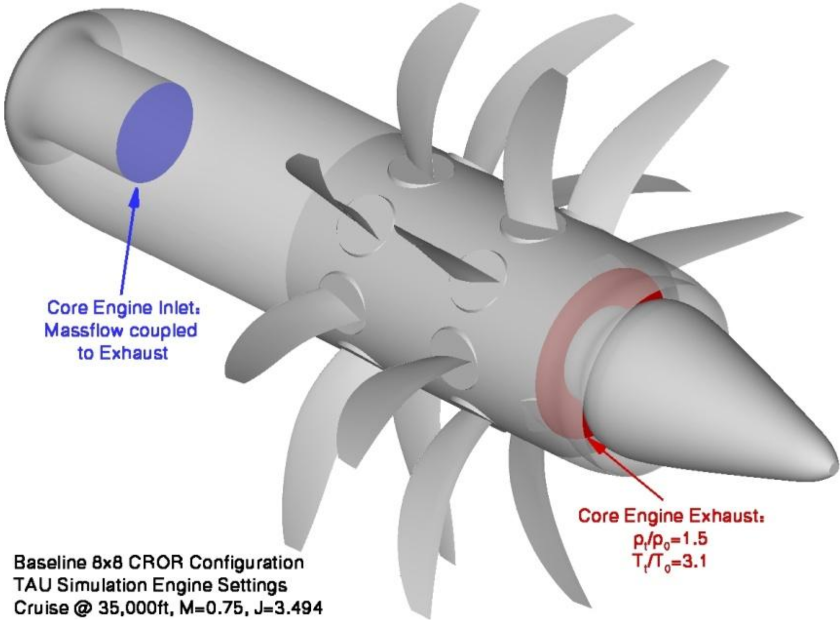

Engine exhaust p_t/p_0	1.5
Engine exhaust T_t/T_0	3.1
$n_1=n_2$ [rpm]	895
$J_1=J_2$	3.494
$\beta_{75,R1}$ [°]	61
$\beta_{75,R2}$ [°]	57.9

CROR Numerical Test Rig: TAU Simulation

- TAU settings: Central Scheme with MD, SAE fully turbulent computation
- Initial steady RANS computation, no prop rotation and all blades pitched to $\beta_{75,R1} = \beta_{75,R2} = 90°$
- Restart from steady solution using Dual Time method with prop rotation and initial blade pitches of $\beta_{75,R1} = 60°$ and $\beta_{75,R2} = 58°$
- Adaptation of blade pitch after 3 prop rotations to obtain a 50:50 thrust split
  - $\beta_{75,R1} = 61°$ and $\beta_{75,R2} = 57.9°$
- Time step variation from dψ=4º/dt to dψ=0.5º/dt with 200 inner iterations
- 6 prop rotations computed on 160 nodes of DLR $C^2A^2S^2E$-cluster
- Runtime ~ 17 days wallclock

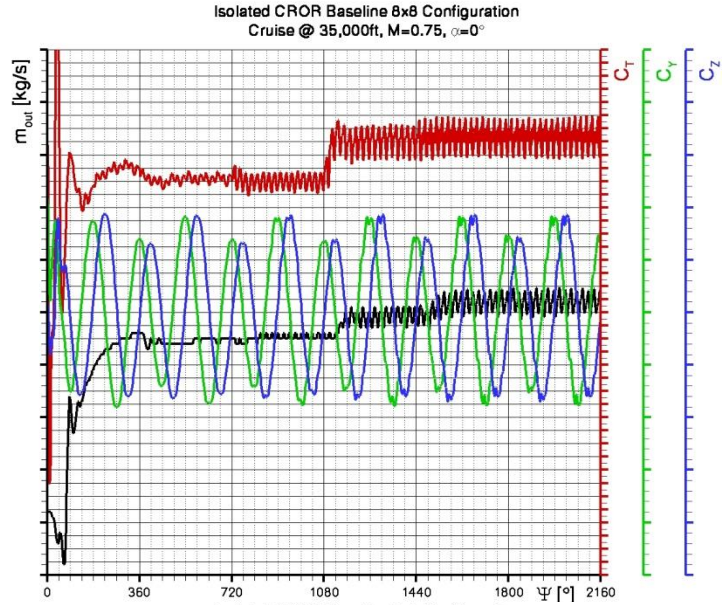

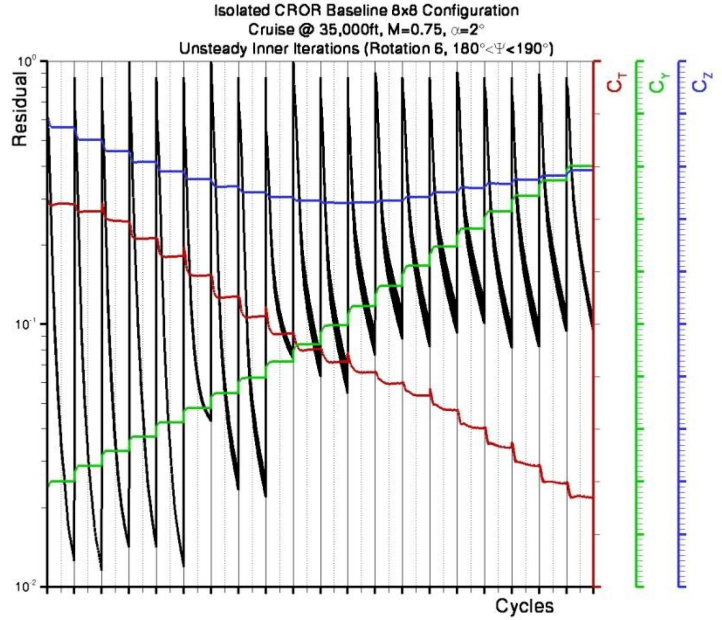

Slipstream Development: Mach Number

- Side view of nacelle with Mach number contours along engine axis
- Transonic flow on nacelle aft of inlet
- Strong unsteady fluctuations and rotor-rotor interactions
- Blade wakes
- Upstream influence of rotors visible
- Angle of attack leads to asymmetry in propeller slipstream with higher velocities in lower half

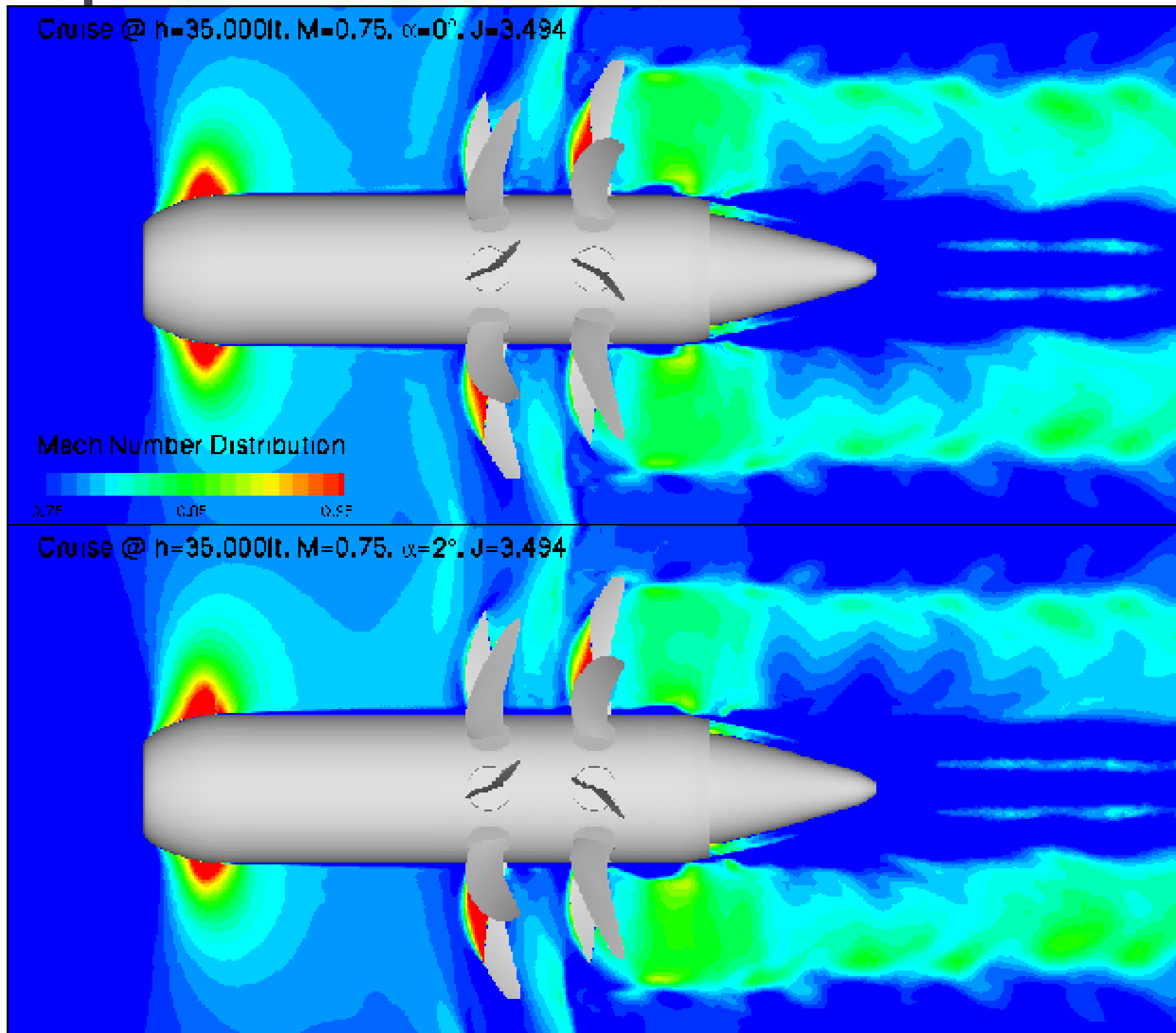

Slipstream Development: Wake Resolution

- Blade wakes quite well resolved
- Influence of aft rotor flow by forward blade wakes
- Generally good functionality of Chimera boundary condition, with smooth transition of contour lines (blade-rotor, rotor-rotor, rotor-nacelle)
- Indication of slight wake dissipation at rotor-rotor Chimera boundary
  - Global mesh density
  - Chimera region mesh density
  - Relative motion (i.e. time-step size)

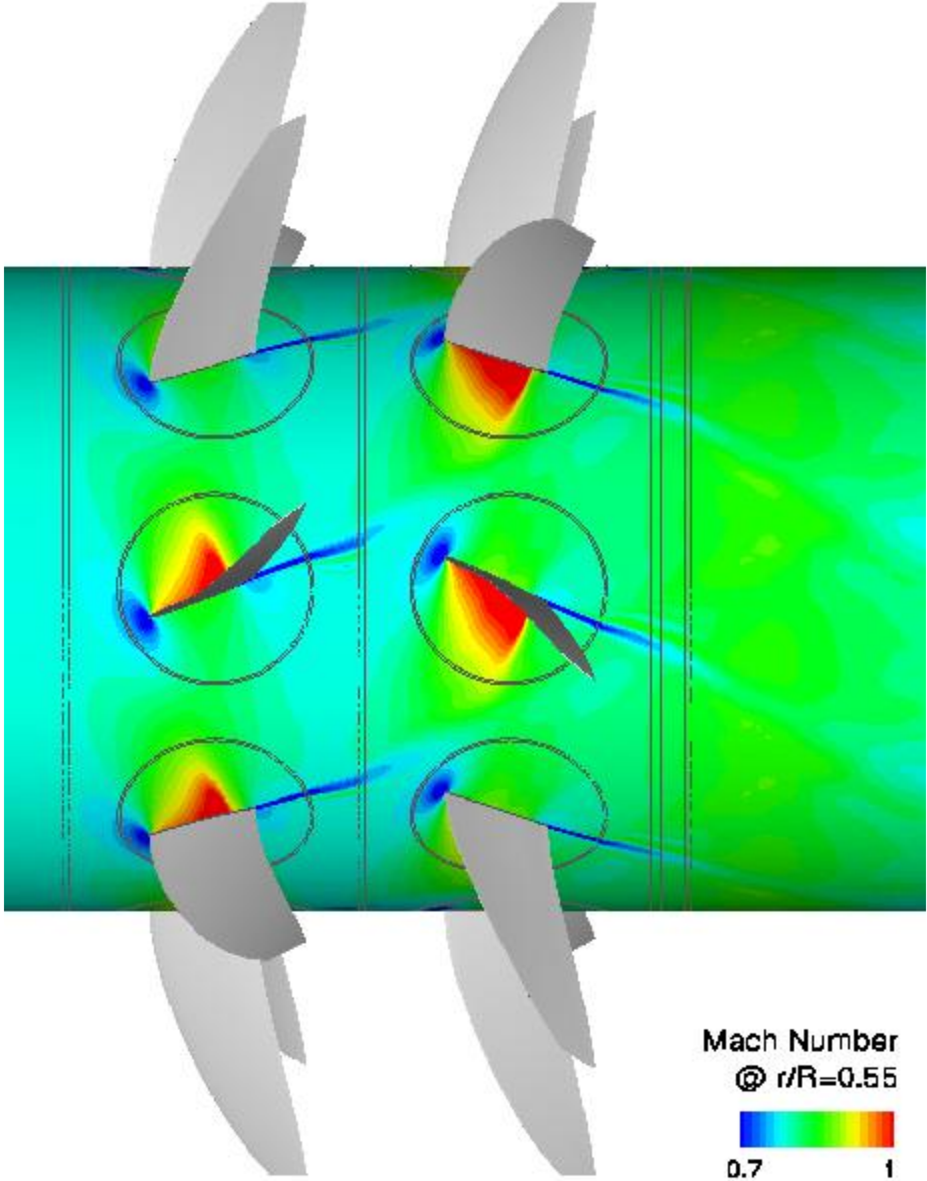

Slipstream Development: Dynamic Pressure @ α=0º

- Top view of nacelle with rays to the left and right at 3 axial positions showing slipstream development
- Symmetrical profiles
- Flow acceleration into first rotor
- Dynamic pressure increases after first and second rotor
- Unsteady fluctuations throughout, with strong impact aft of propellers due to periodic blade wake and tip vortex passage

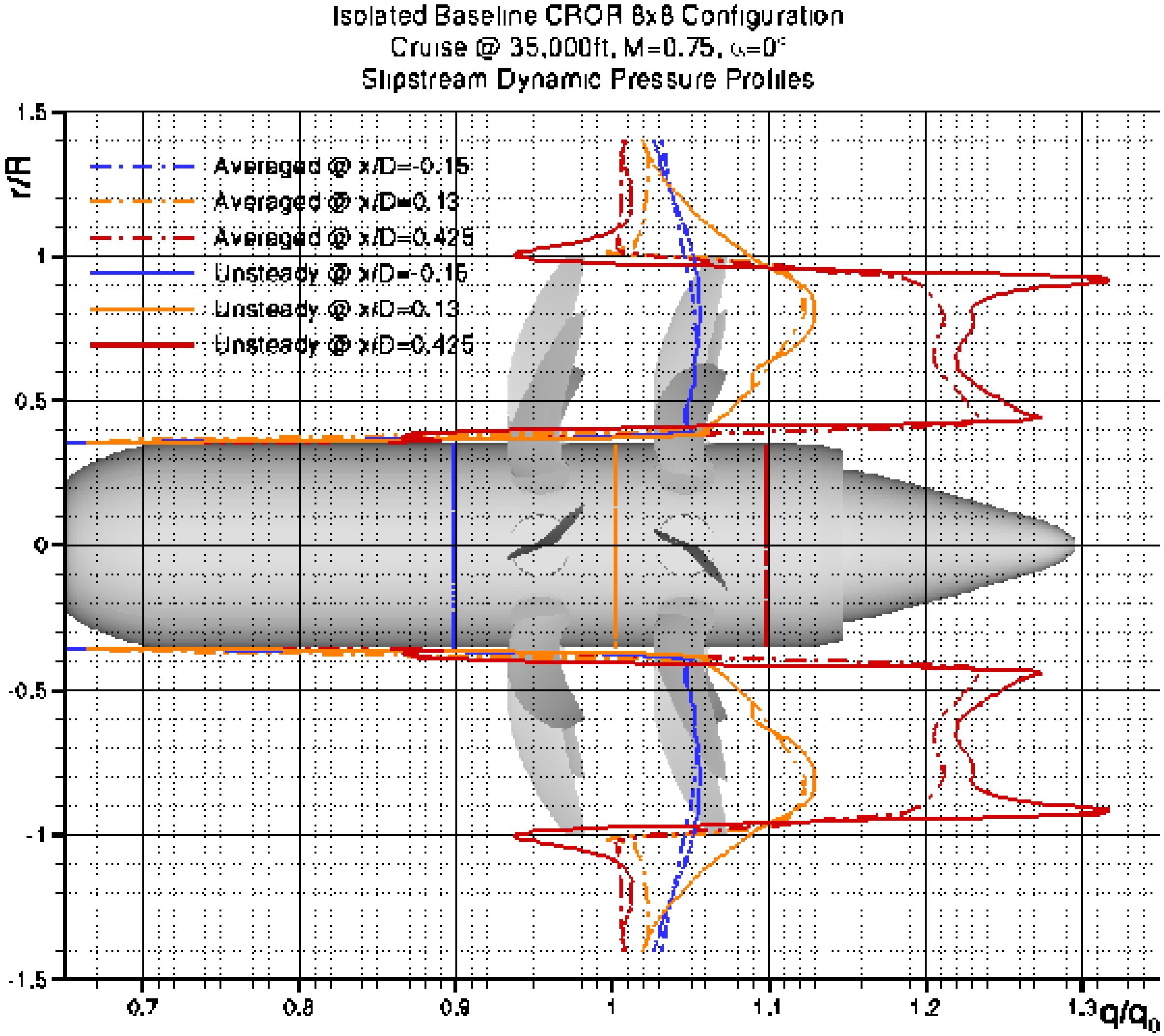

Slipstream Development: Swirl @ α=0º

- Slight oscillations of inflow angle due to upstream effect of rotor 1 flow topology
- Notable swirl losses after the first rotor
- Significant reduction of swirl losses in slipstream through contra-rotating second rotor
- Unsteady fluctuations linked top periodic impact of blade wakes and tip vortices

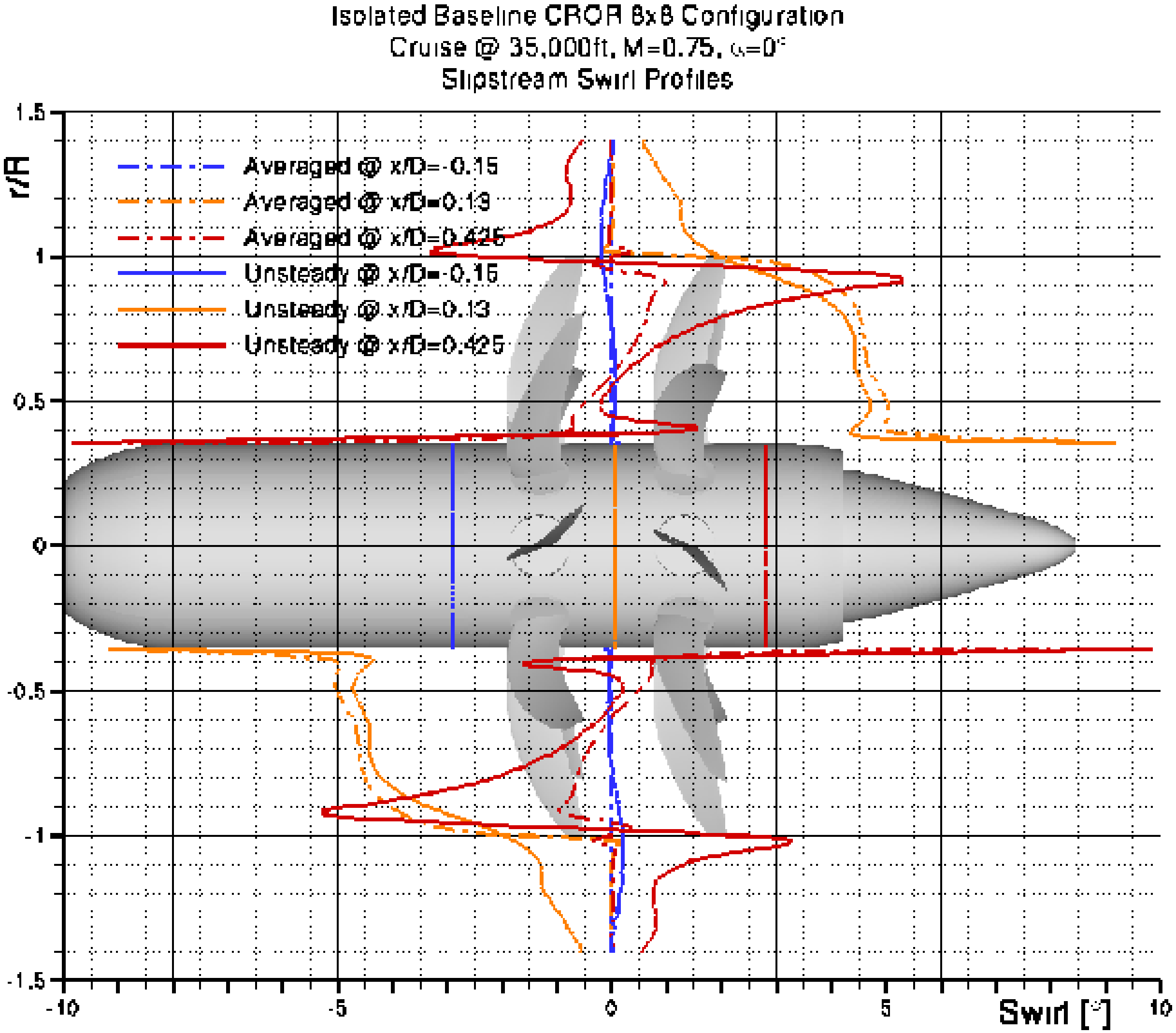

Transonic Flow @ α=0º

- Supersonic flow seen full-span on both rotors blades suction side
- Small patch of transonic flow on blade pressure sides near hub
- Unsteady fluctuations of aft blades transonic flow regions induced by periodic forward rotors blade wake passage

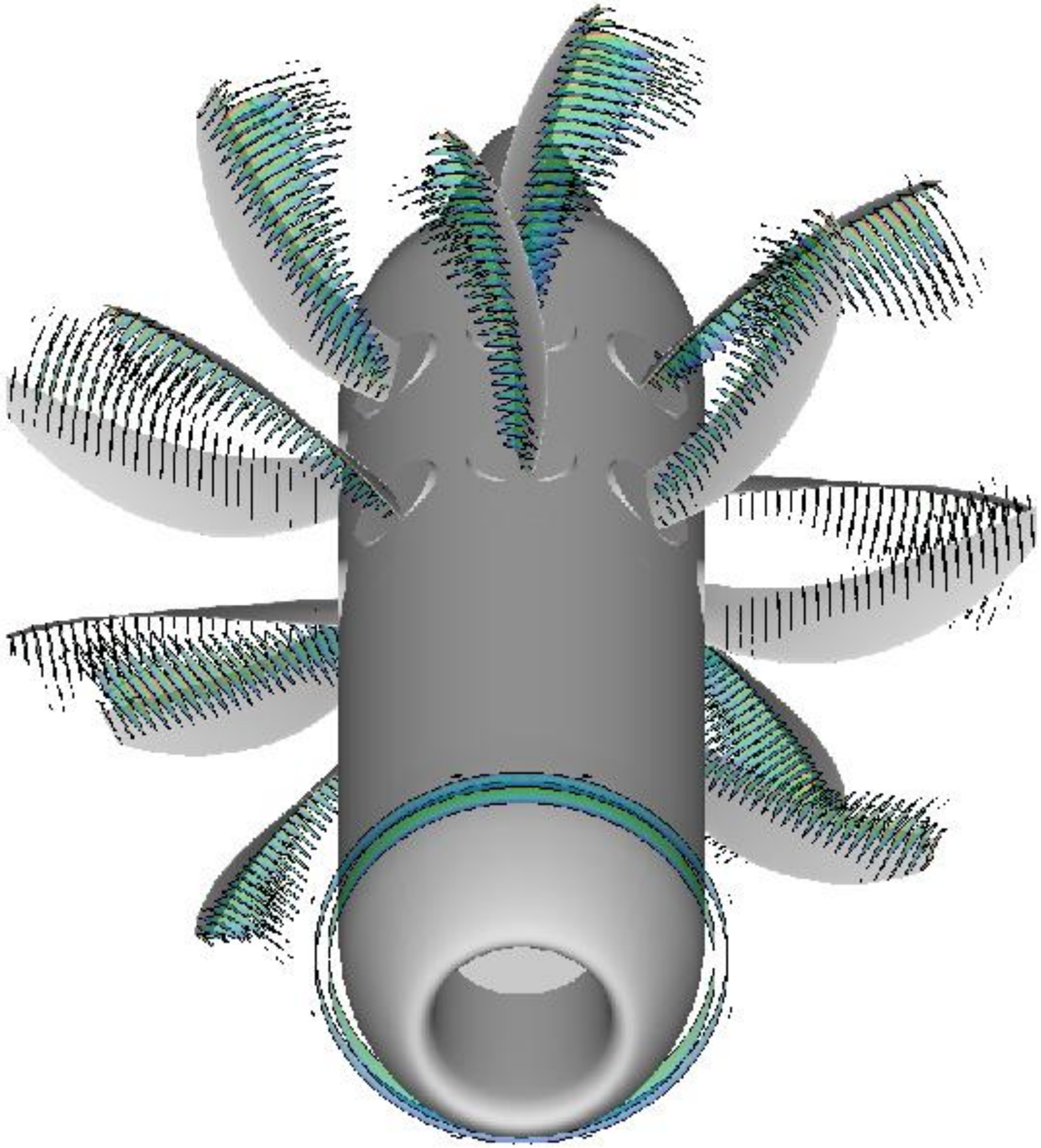

Rotor 2: Blade Pressure Distribution @ α=0º

- Rotor-rotor interactions have pronounced impact on rotor 2 blade pressure distributions
- Unsteady oscillations (16 cycles per rotation) of the pressure distribution visible on pressure and suction side, strongly so at the hub (blade wakes) and tip (blade tip vortices)
- Fluctuation in transonic flow extent and shock intensity

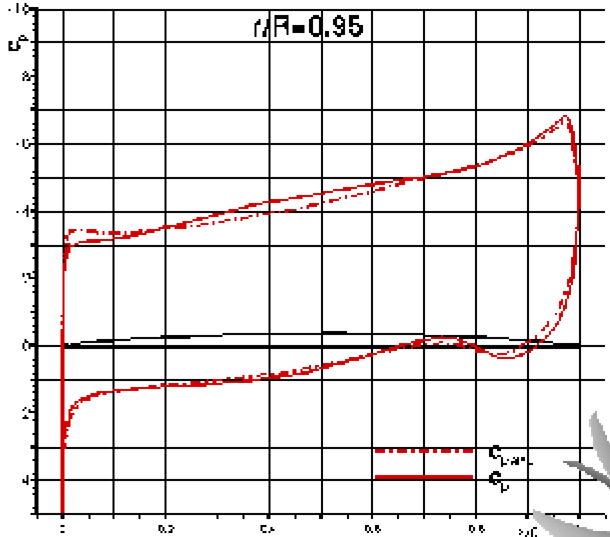

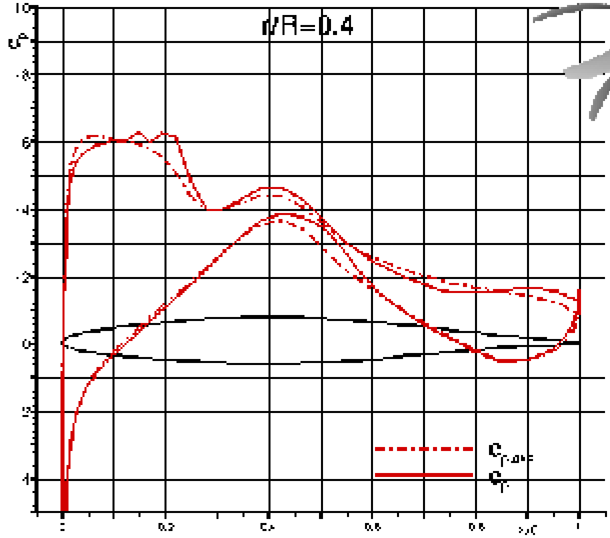

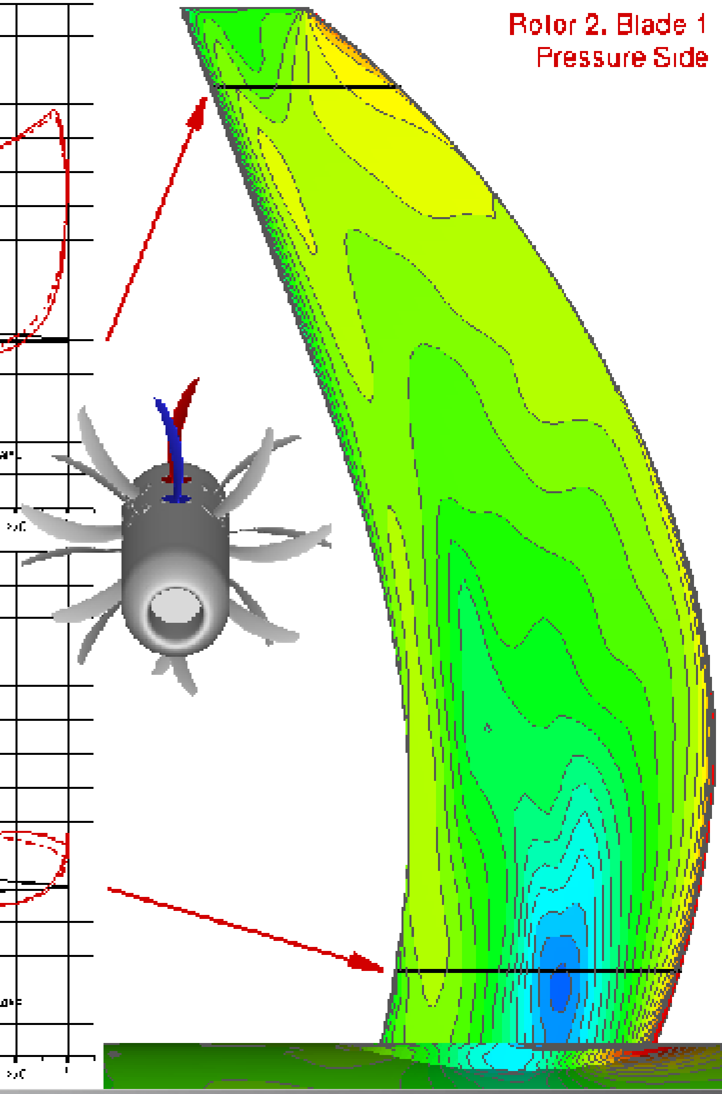

Rotor 1: Blade Pressure Distribution @ α=0º

- Rotor-rotor interactions also have an impact on rotor 1 blades
- Unsteady oscillations (16 cycles per rotation) of the pressure distribution, primarily on the pressure side

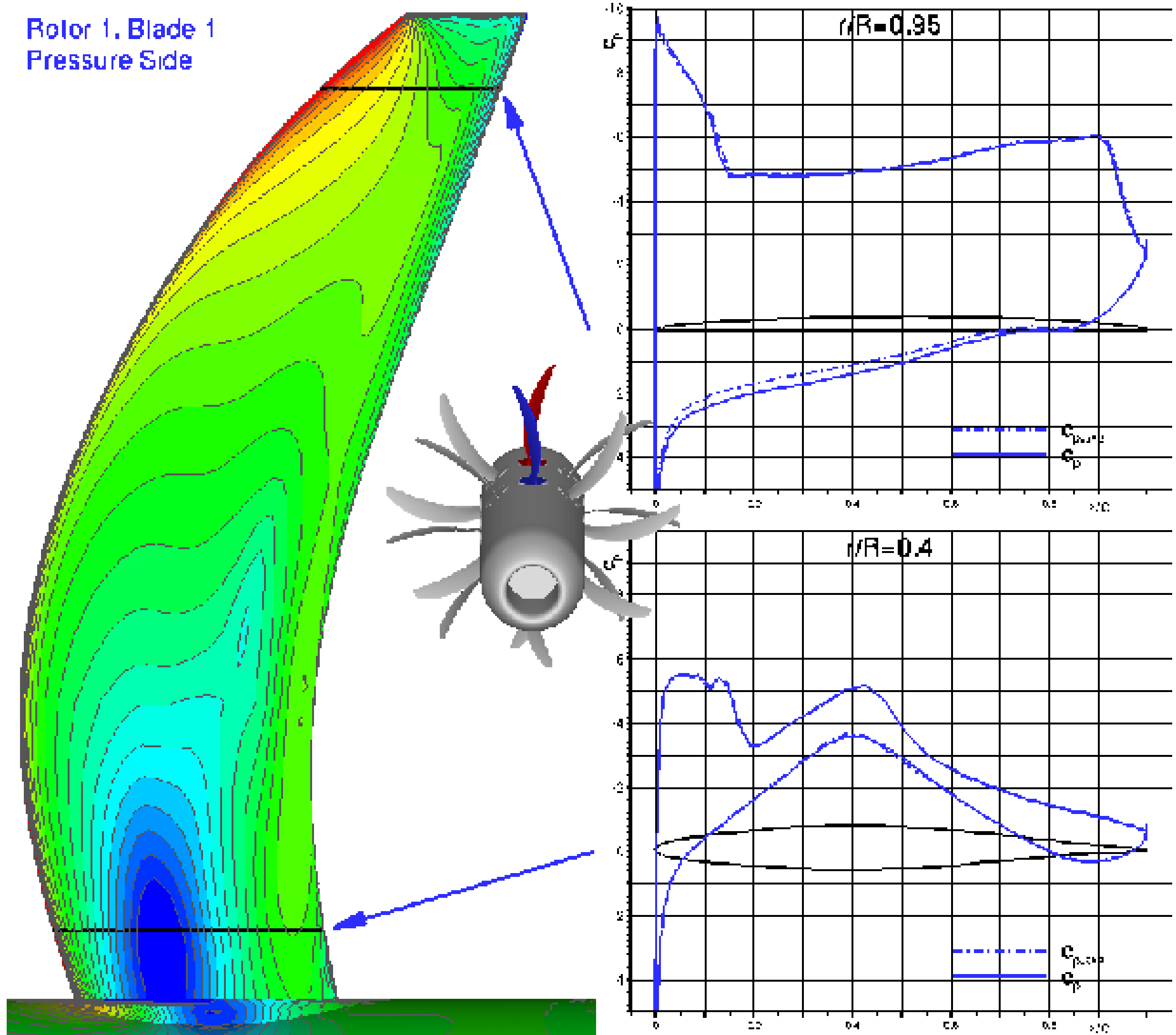

Blade Load Distributions
@ α=0º

- Different blade load distributions
- Blades show 16-cycle force oscillations linked to rotor-rotor blade passage
- Rotor 1 blade wakes lead to full spanwise fluctuations on rotor 2 blades (pronounced at hub and tip)
- Rotor 1 blade shows smaller oscillations

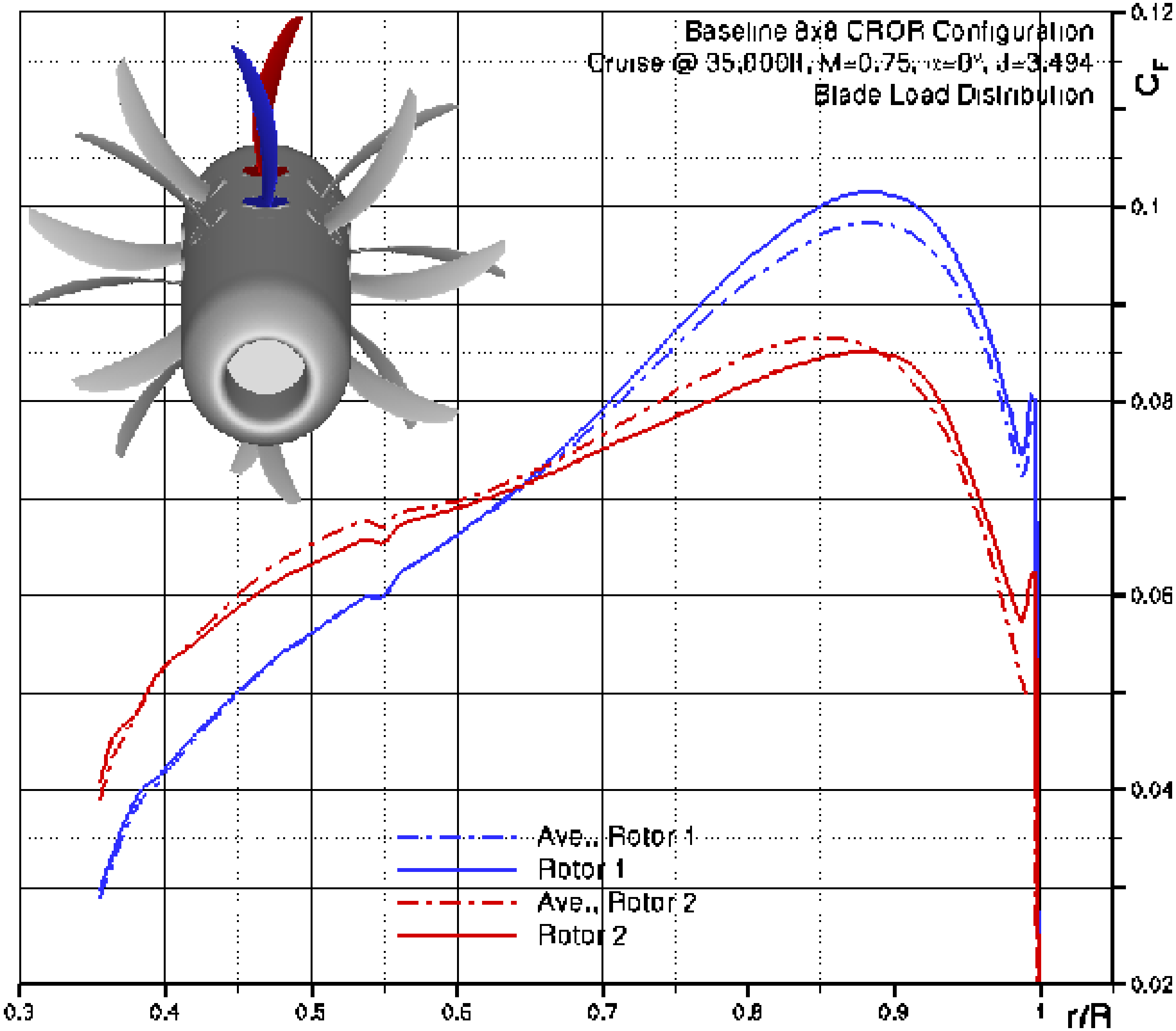

CROR Numerical Test Rig: Blade Force Development

- Cruise at axial flow:
  - 16-cycle periodic oscillations in blade forces during one rotation
  - Larger amplitudes in aft rotor
  - “Constant” mean thrust
  - Sinusoidal lateral and lift forces
- Cruise case at α=2º:
  - 16-cycle periodic oscillations in blade forces during one rotation
  - Sinusoidal thrust development due to AoA influence
  - Modified lateral and lift force development

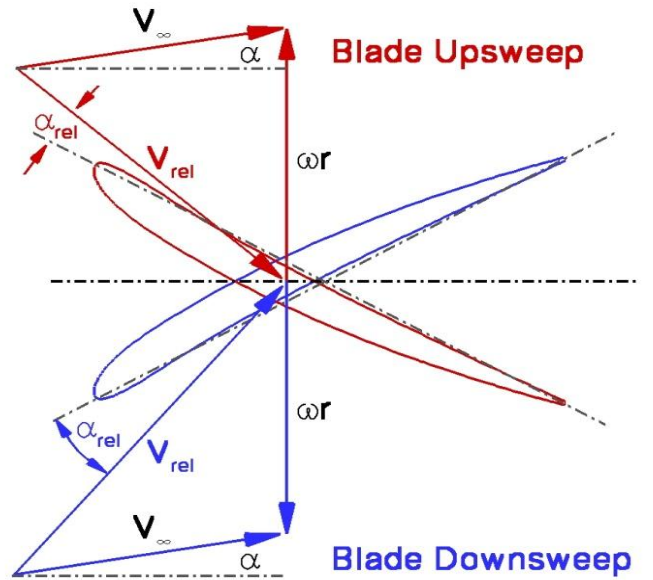

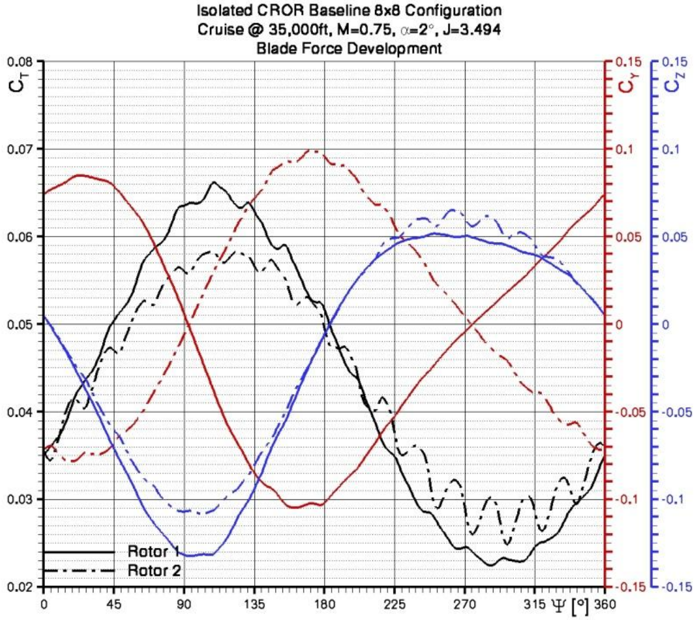

CROR Numerical Test Rig: Rotor Force Development

- Cruise case at axial flow:
  - 16-cycle periodic oscillations persist for rotor thrust, power and efficiency
  - Larger amplitudes in aft rotor
  - 50:50 thrust spilt leads to higher mean power loading in front rotor
  - Better mean efficiency in aft rotor
- Cruise case at α=2º:
  - Retention of same pitch setting leads to higher thrust of front rotor
  - Efficiencies slightly degraded

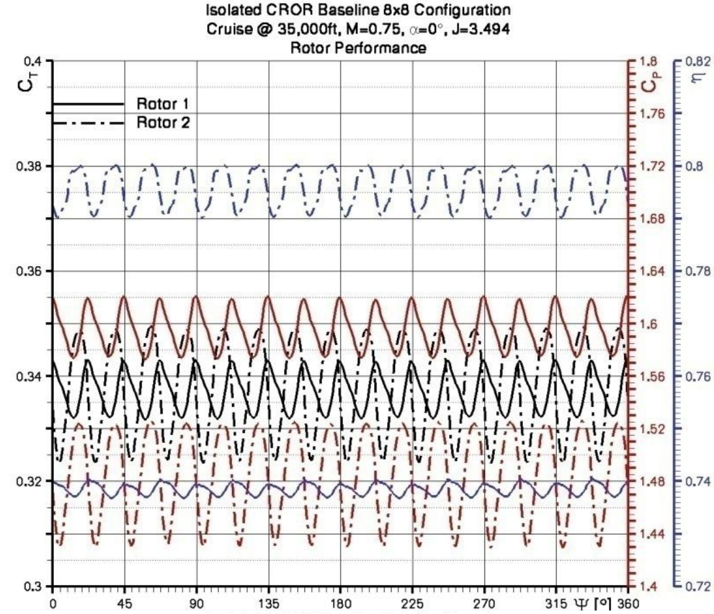

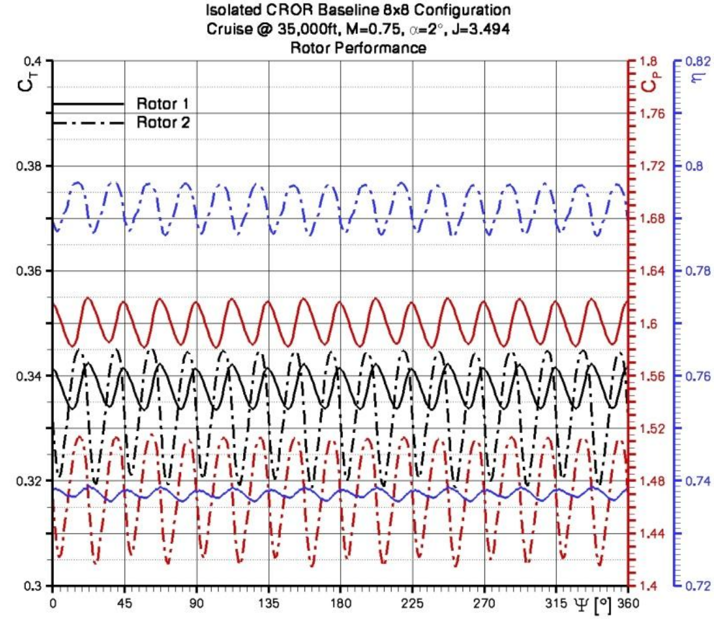

CROR Numerical Test Rig: Mean Blade and Rotor Forces

	Cruise Case @ α=0º			Cruise Case @ α=2º		
	Rotor 1	**Rotor 2**	**Total**	**Rotor 1**	**Rotor 2**	**Total**
F_x [N]	9470.3847	9490.5332	18960.9179	9485.5449	9368.8320	18854.3769
P [kW]	2852.5344	2652.6719	5505.2063	2860.9243	2630.0811	5491.0054
C_T	0.3372	0.3379	-	0.3378	0.3362	-
C_Y	~0	~0	-	-0.055	0.0684	-
C_Z	~0	~0	-	-0.1994	-0.1856	-
C_P	1.5956	1.4838	-	1.6003	1.4712	-
η [%]	73.85	79.58	-	73.75	79.23	-

- Axial flow case: F_x=18.96 kN=4262.583913 lbf
  - $C_{T,R1}/C_{T,R2}$ = 0.9979; $C_{P,R1}/C_{P,R2}$ = 1.0753
- AoA case: F_x=18.85 kN=4238.632544 lbf
  - $C_{T,R1}/C_{T,R2}$ = 1.0125; $C_{P,R1}/C_{P,R2}$ = 1.0878
  - Slight thrust and power increase in R1, decrease in R2
  - Efficiency degrades slightly
  - In-plane forces at AoA, important for engine-airframe integration

CROR Numerical Test Rig: Conclusions & Outlook

- Successful application of high-fidelity uRANS simulation with the DLR TAU-Code to CROR configuration at cruise conditions
- In-depth field and surface flow topology analysis, enhancing understanding of complex aerodynamic interactions
- Outlook:
  - Coupling with Aeroacoustic tools possible & already done with an established approach for SRP and CROR applications
  - Mesh influence studies (density/resolution and Chimera issues)
  - CROR rig parameter studies:
    - As-is: low-speed cases, tip speeds, blade settings (i.e. thrust & power loading splits); rotor-rotor spacing
    - Configuration variations (optimized blade, reduced diameter aft blade, increased blade number in forward rotor, installation effects of pylon)
- Perspective: Maybe modern Hi-Fi CFD and “CAA” can contribute to making Open Rotors work this time around

Propeller/CROR Simulations & $C^2A^2S^2E$:

- Propeller/CROR Simulation & HPC are a “natural go-together”
- Hi-Fi uRANS CFD of propeller/CROR configurations offers great potential for analysis and design, benefitting a number of disciplines (aerodynamics, aeroacoustics, structures)
  - Yes, it’s not always necessary to run rotating propeller unsteady CFD where simpler methods can suffice, but certain smartly chosen simulations are invaluable
- HPC in the form of the $C^2A^2S^2E$-cluster is an enabler, allowing for increased fidelity with reduced turn-around times
- Web-find of “Final Challenge” on CROR noise mitigation in a 2007 NASA GRC presentation
- Thanks to $C^2A^2S^2E$ capability of just being able to run big simulations, perhaps an answer to this challenge can be found

- Now all I need is more disk space…